Quartz diorite (FR–24)

Texture: Equigranualr.

Constitutent minerals: The order of distribution of main minerals is the following; plagioclase > quartz > hornblende > biotite ≫ potash-feldspar. Plagioclase is 0.4 – 3.2mm in size and euhedral or subhedral, and remarkably altered to sericite, epidote and sphene. Quartz is 0.4 – 2.6mm in size and potash-feldspar 0.6 – 2mm, and both show an anhedral form. Mafic minerals consist of hornblende and biotite: the former 0.4 – 2.4mm in size shows a euhedral or subhedral form and no alteration, the latter 0.5 – 2mm in length shows a subhedral or anhedral form and most of all are altered completely to chlorite and sphene.

Diorite (WR–179)

Texture: Equigranualr.

Constituent minerals: Primary minerals are composed mainly of plagioclase and hornblende, showing a remarkable alteration. Particularly, plagioclase is mostly altered to sericite. Hornblende is changed to chlorite and opaque minerals. On the size of crystals, plagiocalse is 1 – 3mm and hornblende 0.4 – 1.6mm. Other secondary minerals such as prehnite, calcite and albite are also observable, forming veinlets.

Photo-characteristics: Because the scale of exposure is very small, the characteristics on these rocks were hardly recognizable. Moreover the resistance of these rocks is almost same as the host rocks, and it is difficult to distinguish them from other rocks.

Age: The results of the age determination on 2 samples of quartz diorite gave ages of 30.4 ± 0.9m.y. and 40.2 ± 6.8m.y. These ages indicate the rock is from the Eocene to Oligocene period. This does not constradict the fact that these rocks led the contact metamorphism in the limestone of the Sablayan group, which is considered to be of Eocene age, and that these are uncomformably overlain by the Bongabong group.

1–5–3 Basic rocks

Dolerite and gabbro exist in the area as small scale dikes.

Distribution and rock facies: Dolerite is distributed in the central sections of this area. It intrudes into the Lumintao and Mansalay formations and it mostly strikes N–S. The width is generally less than 10m, and at its largest does not exceed 100m. These are massive fine-grained rocks, which appear greyish green to dark green in color.

Gabbro is found in the ultramafic rocks and the surroundings. The rock appears dark green to dark grey in color, and is medium to coarse-grained massive rocks, which is formed of plagioclase and pyroxene.

The results of microscopic observations are as follows;

Dolerite (YR–20)

Texture: Subophitic texture.

Constituent minerals : Euhedral plagioclase 0.4 – 1mm in size being a lathlike form and anhedral to subhedral augite with 0.2 – 1.5mm in size. Chlorite are filling spaces those crystals. Plagiocalse is altered to chlorite in a vermicular form, and some of mafic minerals are completely changed to chlorite or opaque minerals.

Gabbro (YR–05)

Texture: Equigranualr.

Constituent mineals : The order of distribution of main minerals is the following; plagioclase > augite ≫ hypersthene. Plagioclase is subhedral or anhedral and 0.3 – 2.5mm in size, and contains a 50 – 70% of An component. Augite is 0.4 – 1.4mm in size and hypesthene 0.4 – 0.6mm, and both show a anhedral form. On secondary minerals, chlorite is observed along the fracture of pyroxene and albite as well as chalcedony are also observable.

photo-characteristic: The rocks are small scale dikes and exhibit the almost same resistance as host rocks. Consequently, it is difficult to discriminate them on an aerial photograph.

Age: It is thought that the age of the dolerite is the same as that of the Lumintao formation, and the age of the gabbro is the later stage of activities of the ultramafic rocks.

1–6 Chemical composition of the rocks

A total of 14 samples were analyzed for their chemical composition: 6 samples from the Halcon metamorphics, 1 sample each from the basalt of the Baco group and the Mamburao group, and 6 samples from the intrusive rocks. The results of these analyses and the normative composition are shown in Table 1–4.

On the Halcon metamorphics, analyses of gneiss, green schist, and amphibolite were

carried out. These values were plotted on an ACF diagram (Fig. I–9A). On the diagram, the data from the gneiss samples fall in the field of greywacke and pelitic rock, while the samples of amphibolite and green schist (which exclude sample FR–103) are in the field of basic igneous rocks. However, sample FR–103 was plotted in the middle of both, and this feature is supported by the fact that the coexisting of chlorite and muscovite in this sample is recognized under the microscopic examination. When the normative composition of the samples of gneiss were plotted onto the Q–Pl–Kf diagram (Fig. I–9B), both of the samples enter the area of granodiorite.

As for the basalt of the Baco group and the Mamburao group, the former includes nepheline and olivine as normative minerals, and is alkalic, while the latter includes hypersthene without the above normative minerals. However, on the (Na20+K20)–SiO_2 diagram (Fig. I–9C), both enter the area of the alkaline rocks. It shows that these basalts are characterized by geosynclinal volcanic rocks. In comparizon with the data of other areas on the diagram, the above samples show the similar values to the average values of alkali basalt in oceanic islands and seamounts and in Circum-Japan Sea alkali province by Tomita (1935), moreover, these are plotted in the part of higher alkali content within the field of Cretaceous green rocks composed mainly of basalt in the Shimanto belt, Japan. These features are also recognizable on AMF diagram (Fig. I–9D).

On the analyzed values of the quartz diorite, sample FR–41 shows a trend of low amounts of Fe_2+, Fe_3+, and K_2O, while being rich in Al_2O_3 and Na_2O, and sample FR–24 shows trends of being poor in CaO, while being rich in MgO. In between both, the differences in Na_2O/K_2O are distinct. Plotting these normative compositions onto a Q–Pl–Kf diagram (Fig. I–9B), sample FR–41 falls in the field of tonalite in the granitic plutonic rock, while sample FR–24 enters the field of quartz monzo-diorite.

The values for gabbro are similar to those obtained from the gabbro exposed in Solsona on the Luzon Island (JICA, 1981), and the abundance of Al_2O_3 and CaO are characteristics of both.

From the results of the ultramafic rocks it is recognized that, MgO is rich, and the Mg/Fe values (atomic comparison) is large at 8.2 to 12.4, and the H_2O^+ is characterisitcally abundant. Also, when these values were plotted on the Fe/(Fe+Mg)–Mg/Si diagram (Fig I–9E), the samples from this study occupies almost the same field as the Horoman peridotite body of the Hidaka metamorphic zone of Japan, which is an alpine type.

Table I-4 Chemical Composition and C.I.P.W. Norm

Group Name		Intrusive Rocks						Baco G.	Mamburao G.	Halcon Metamorphics					
Sample No.		FR-41	FR-24	YR-05	SR-65	FR-06	SR-38	FR-15	FR-17	FR-39	FR-113	FR-103	WR-12	SR-90	YR-12
Location		Camarong River	Mamburao River	Amnay River	Bansud River	Paluan	Amnay River	Binunangin River	Banilad Creek	Comarong River	Agbuyi Creek	Alog River	Bongabong River	San Teodoro	Rayusan River
Rock Name		grano-diorite	quartz diorite	gabbro	harzbur-gite	serpenti-nite	serpenti-nite	basalt	basalt	gneiss	gneiss	green schist	green schist	green schist	amphibo-lite
Chemical composition	SiO_2	71.27	58.81	47.89	40.12	38.48	33.51	46.37	50.52	72.64	70.18	62.42	50.38	45.24	50.84
	TiO_2	0.19	0.74	0.21	0.02	0.03	0.01	2.82	1.73	0.18	0.35	0.65	1.48	1.45	1.04
	Al_2O_3	16.13	16.62	20.55	1.52	1.76	0.80	15.20	15.77	15.02	15.24	14.90	15.21	15.34	15.92
	Fe_2O_3	0.59	2.56	0.84	4.12	6.99	4.35	4.87	5.99	0.52	0.51	3.44	2.80	2.24	2.38
	FeO	1.08	3.81	4.92	3.70	1.11	1.90	5.93	5.68	1.37	2.19	3.16	7.83	8.73	6.97
	MnO	0.02	0.10	0.12	0.12	0.12	0.09	0.13	0.22	0.06	0.06	0.16	0.18	0.21	0.16
	MgO	0.35	3.84	7.75	38.65	34.19	40.32	3.94	3.77	0.84	1.47	2.44	6.91	8.08	7.08
	CaO	2.92	3.87	13.93	1.21	4.60	2.02	9.81	7.65	1.57	2.41	5.07	11.16	8.83	10.48
	Na_2O	5.07	4.09	1.89	0.02	0.02	0.02	4.68	4.60	4.61	4.45	1.43	2.50	2.44	2.68
	K_2O	0.83	2.68	0.06	0.01	0.01	0.01	1.10	1.16	1.54	1.14	2.81	0.18	0.62	0.66
	P_2O_5	0.14	0.20	0.02	0.01	0.01	0.01	0.63	0.31	0.08	0.11	0.18	0.16	0.15	0.10
	CO_2	–	0.11	–	–	–	0.57	2.02	–	–	–	0.66	–	2.27	–
	H_2O+	0.65	1.74	1.57	9.89	12.01	15.52	2.20	2.18	1.00	1.15	1.94	0.97	4.15	0.87
	H_2O-	0.04	0.08	0.02	0.22	0.43	0.68	0.14	0.22	0.06	0.04	0.06	0.12	0.14	0.04
	total	99.28	99.25	99.77	99.61	99.76	99.81	99.84	99.80	99.49	99.30	99.32	99.88	99.89	99.22
CIPW norm	Q	31.66	9.86						0.47	34.67	31.46	30.16	2.16		0.43
	C	1.92	0.69							3.11	2.57	2.25		0.22	
	or	4.91	15.84	0.35	0.06	0.06	0.06	6.50	6.86	9.10	6.74	16.61	1.06	3.66	3.90
	ab	42.90	34.61	15.99	0.17	0.17	0.17	38.05	38.92	39.01	37.65	12.10	21.15	20.65	22.68
	an	13.57	17.20	47.41	4.03	4.68	2.06	17.22	18.96	7.27	11.24	19.80	29.75	28.48	29.46
	ne							0.84							
	wodi			9.00	0.80	7.55	1.79	6.08	7.09				10.26		9.14
	endi			5.88	0.67	6.52	1.55	4.42	4.92				6.16		5.61
	fsdi			2.50	0.02			1.10	1.59				3.56		3.00
	enhy	0.87	9.56	3.92	25.94	16.58	3.37		4.47	2.09	3.66	6.08	11.05	17.34	12.02
	fshy	1.22	3.85	1.67	0.96				1.45	1.90	3.13	2.19	6.39	10.49	6.42
	fool			6.66	48.81	43.48	66.93	3.78						1.95	
	faol			3.12	2.00		0.03	1.04						1.30	
	mt	0.86	3.71	1.22	5.97	3.88	6.31	7.06	8.68	0.75	0.74	4.99	4.06	3.25	3.45
	hm					4.31									
	il	0.36	1.41	0.40	0.04	0.06	0.02	5.36	3.29	0.34	0.66	1.23	2.81	2.75	1.98
	ap	0.32	0.46	0.05	0.02	0.02	0.02	1.46	0.72	0.19	0.25	0.42	0.37	0.35	0.23
	cc		0.26				1.35	4.78				1.56		5.37	
	total	98.59	97.45	98.17	89.49	87.31	83.66	97.69	97.42	98.43	98.10	97.39	98.78	95.81	98.32
	D.I.	80.61	61.89	16.64	0.26	0.26	0.27	45.60	47.47	84.10	77.32	60.45	24.67	25.37	27.47

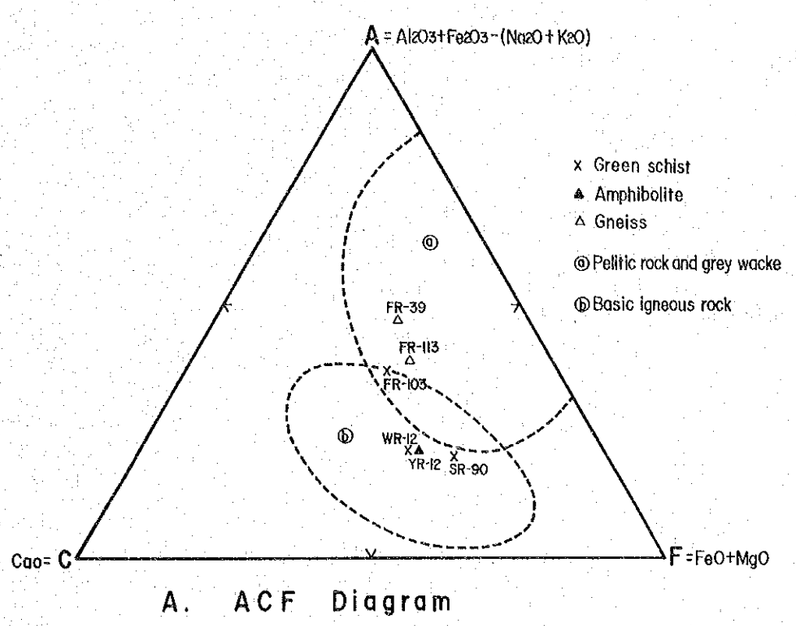

A. ACF Diagram

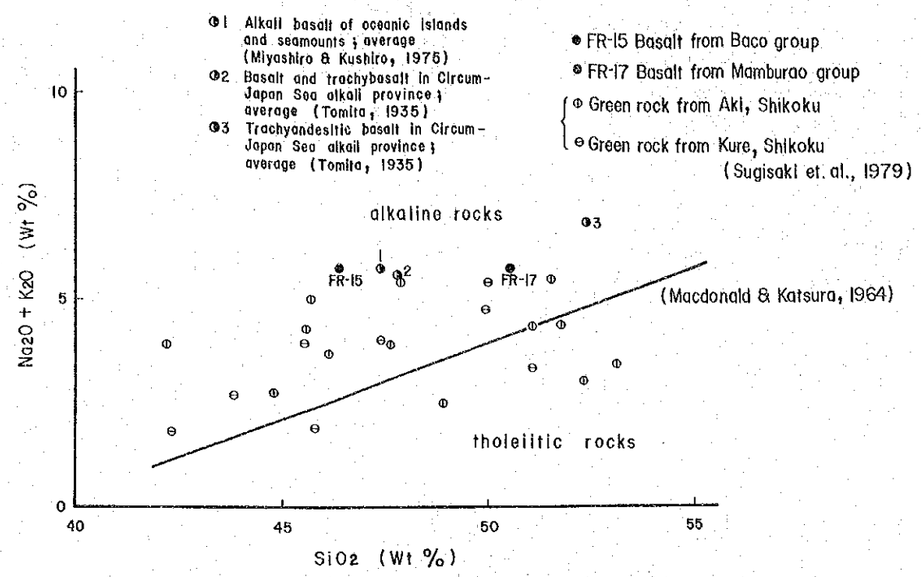

C. $(Na_2O + K_2O) - SiO_2$ Diagram

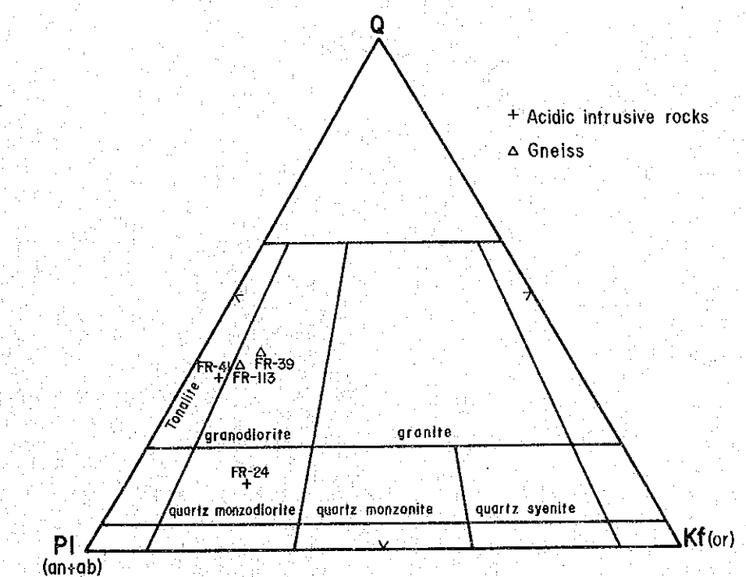

B. Q-Pl-Kf Diagram

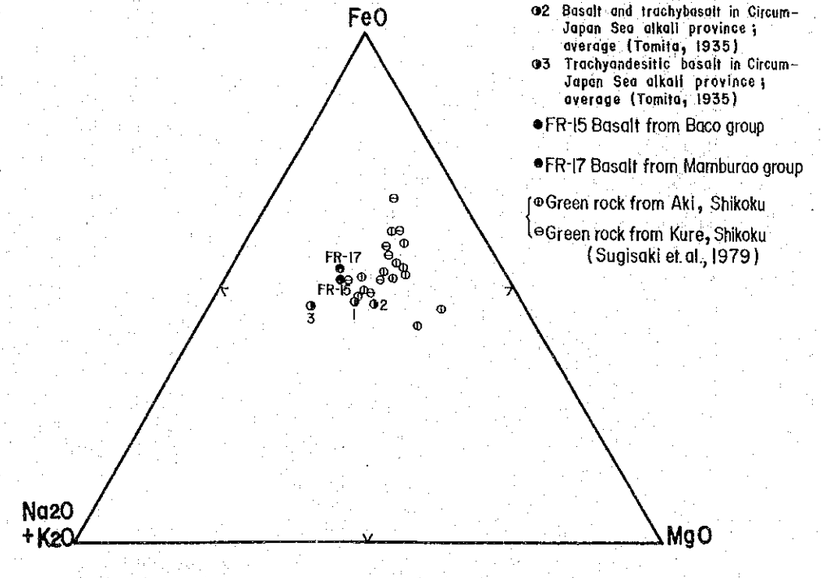

D. AMF Diagram

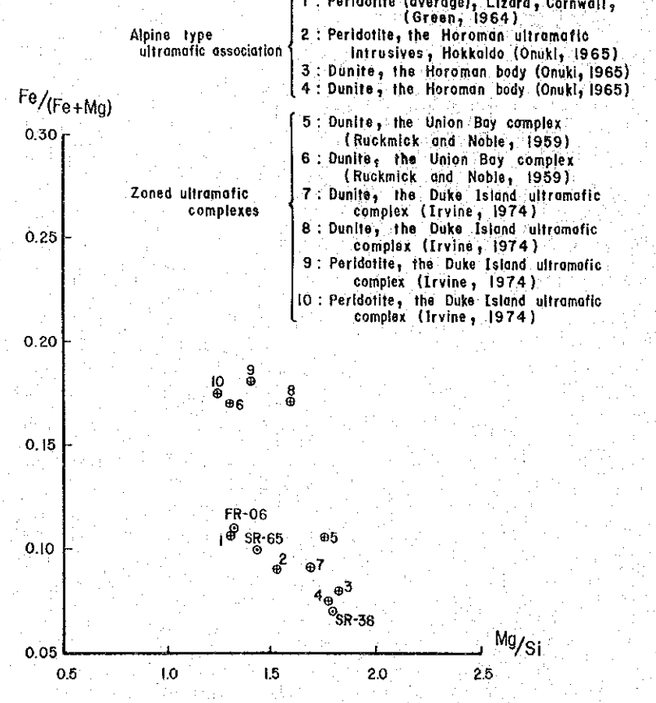

E. Fe/(Fe+Mg) - Mg/Si Diagram

Fig. I-9 Diagrams of Chemical Composition

1–7 Geological Structure and Geological History

1–7–1 Geological Structure

The survey area can be divided into five zones : that is ① Central lift zone, ② Paluan lift zone, ③ Mamburao basin, ④ Southwestern basin and ⑤ Eastern basin (Fig. I–10).

The Central and the Paluan lift zones, which build the mountain range in Mindoro Island, are composed of Halcon metamorphics and are separated by Mamburao basin. The Mamburao, the Southwestern and the Eastern basins are filled by a series of Cenozoic sediments ranging from the Mamburao to the Socorro groups and make up the low lands. Large-scale faults and ultramafics intrusion are found near the boundary between the lift zone and the basin.

As is evident from the distribution of tectoniczones and the geological sections, the island, as a whole, shows a large anticlinal structure trending NW–SE. The following three systems of the structure can be recognized in the area.

① NNW–SSE System

This system is the most remarkable one as shown by the elongation of the island.

This system is recognizable in the whole island on the structures such as fault, fold, general strike of the sedimentary groups and intrusive rocks. The typical faults are Mindoro fault (tentatively proposed) extending over 80km and Wasig fault (Teves, 1953) extending over 40km, both of which are eastside-slipped gravity faults, bordering central lift zone from Eastern basin. In the east of Sablayan, there is a fault with the same system which is steep and is westside-slipped gravity fault. As for folding, the Sablayan group and the Socorro group distributed in the southern area have a folding structure with an axial length of 2 ~ 10km and a wave length of 1 ~ 2km. In the Halcon metamorphics there is a folding axis with longer wave length on the extension of Mindoro fault, plunging toward south. The intrusive rocks extending toward NNW are mostly ultramafic rocks and with some quartz dioritic and gabbroic dikes. The forming age of the structure is considered to start after Cretaceous and continue until Pleistocene in which the movement was most active.

② NE–SW system

This system can be found in the direction of folding, fault and some intrusive rocks. There are two types of folding, one of which is developed in the Baco group, having a wave length 1 ~ 2km in the southeast and 10km in the central part with all axes lengths of 3 ~ 10km. The other type is newly developed in Mamburao basin, being in a larger scale with a wave length extending over 15km and an axial length of over 30km. The most characteristic

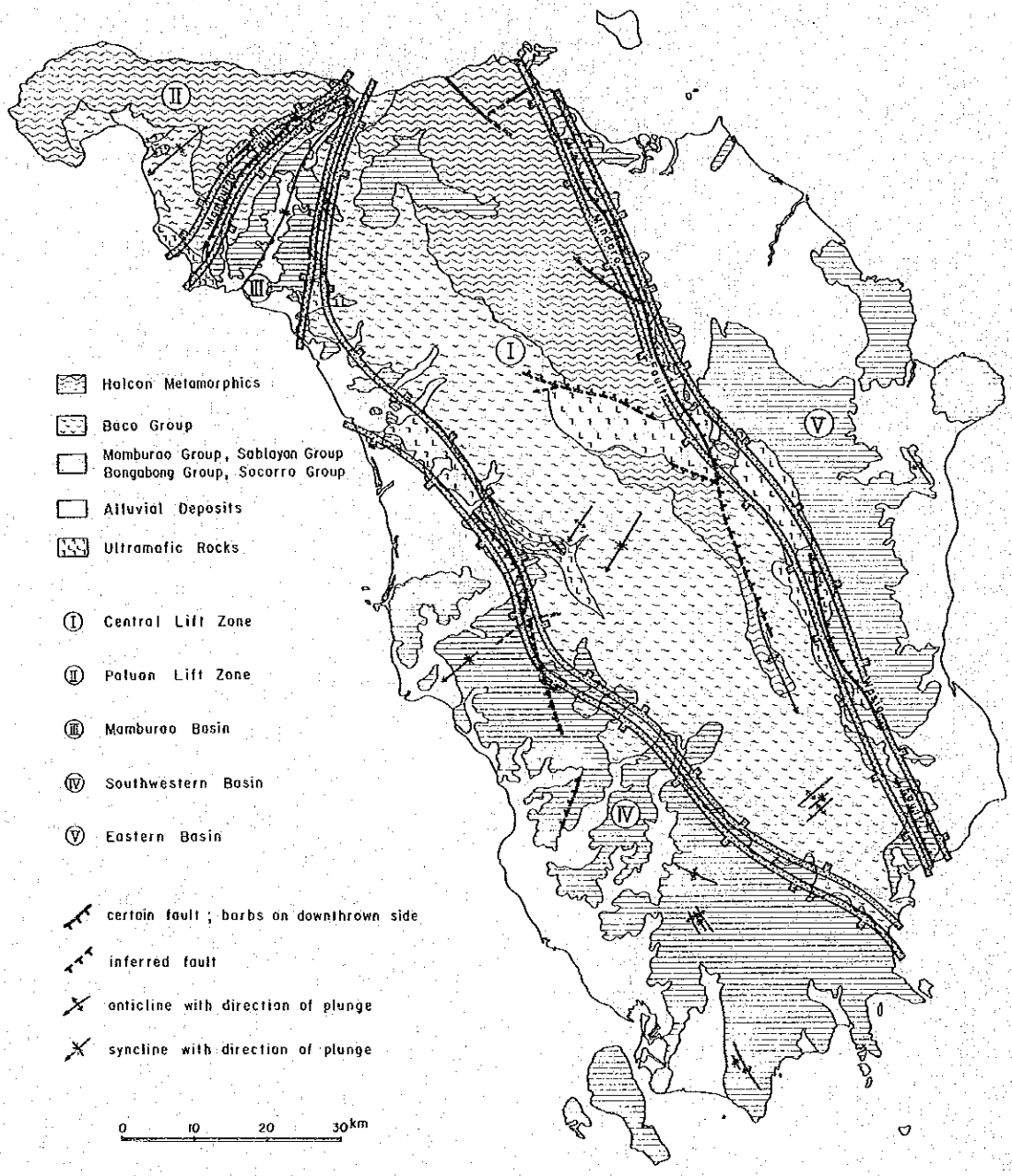

Fig. Ⅰ-10 Tectonic Map of the Survey Area

fault of this system is Mamburao fault (tentatively proposed) which is an eastside-slipped gravity fault with an extension of 25km, bordering Mamburao basin from Paluan lift zone. The movements are presumed to occur after the sedimentation of the Baco group of the end of Jurasic to early Cretaceous and after sedimentation of the Sablayan group of Miocene to Pliocene.

③ WNW–ESE system

This system can be seen on the faults developed in the Halcon metamorphics distributed along the Mindoro fault. Some of these faults have been cut by the Mindoro Fault and have controlled the ultramafics intrusion.

The lengths of these faults range from 10 to 15km, tending northside slip in the north and southside slip in the center to the south.

This system may have been formed before or after the ultramafic intrusion, namely in Cretaceous.

1–7–2 Geological history

The Halcon metamorphics, basement of the island, was formed by regional metamorphism caused by the structural movement of late Paleozoic. As is evident from the unconformity between the Halcon metamorphics and the Baco group, early Mesozoic was at the stage of erosion. In Jurassic a large-scaled marine transgression started and formed the sedimental basin where the Baco group was deposited. The basin is characterized by different deposition, that is, deposition of thick sandstone and mudstone with some igneous activities in the early stage and deposition of thick basalt lava erupted by vigorous igneous activities in the later stage.

In the Cretaceous period, the area became land as a result of uplifting which formed folding structures with a NW–SW system and imposed weak metamorphism on the northern to the central area. But the movement was differential, so that the fractures of NNW–SSE and WNW–ESE systems were gradually developed between blocks with different movement, which led to the intrusion of ultramafics and basic rocks.

During Tertiary period, marine transgression and retrogression were repeated and the neritic Mamburao, Sablayan and Bongabong groups were deposited. The differential uplifting in this period was so distinct that the sedimentary basin split into two (east and west sides) across the central portion, resulting in some differences in rock facies deposited. That is,

the west side is characterized by limestone and conglomerate with few volcanic rocks, on the contrary, the east side, by taffaceous mudstone-siltstone and sandstone with much volcanic rocks.

Acidic-intermediate dikes were intruded near the boundary between two blocks with different movement. Contrary to the Tertiary system stated above, the sedimentary basin of the Socorro group deposited chiefly in Quaternary was almost continental except that of reef limestone.

The structure of a NNW–SSE system formed by uplifting which started from Cretaceous, had become more clear during Miocene and Pleistocene period, and appeared as the Mindoro fault, the Wasig fault and some foldings. With almost the same time, a synclinal structure with a NE–SE system and the Mamburao fault were formed in Mamburao area.

Chapter 2 Ore Deposits

2–1 General Remarks

As shown in Fig. I–11 and Table A–5 there are numerous known ore deposits in Mindoro Island. As reflected in the name of the island (Mina de Oro = Mindoro), gold ore deposits are famous, and the mining of alluvial gold is very extensive in the area of San Teodoro in the northeastern part. Nickel-chrome ore is found in the ultramafic rocks along the geological structural line, and in one part an investigation covering a wide area was carried out, the object of which was focussed on nickeliferrous laterite. Iron ore deposits can be found near the mountain summits of the northern parts of the central mountains, and are considered to be contact metasomatic ore deposits existing in limestone, which uncomformably covers the Halcon metamorphics. The main ore body is made up of magnetite, and includes hematite.

Copper ore deposits can be seen together with the acidic igneous rock which is scattered along the Mindoro fault which runs along the eastern side of the central mountain range.

As for non metal ore deposits, there are barite deposits which originate in the Mesazoic formation of the southern parts as well as coal deposits of the Tertiary Period. At this time mining is being carried out in the Barite deposits.

In Puerto Galera, small scale marble deposits can be found in the rock formations of the Halcon metamorphics.

2–2 Summary of Each Ore Deposit

A summary of the characteristics of each type of ore deposit obtained from the present study is as follows.

2–2–1 Gold ore deposits

According to some recent unpublished data from the BMG, alluvial gold in Mindoro Island is being produced at a rate of 50g/day in the eastern parts, and 10g/day in the western parts, the number of panners engaged in these operations is said to be 80 and 40, respectively.

(A) The eastern area

Alluvial gold is mined extensively in both the San Teodoro and Puerto Galera Rivers in the northeast parts, and Binaybay, located in the middle reaches of the Liano Cawayan River is an especially famous production site. This alluvial gold is mixed with the sedimentary materials deposited in the river beds that traverse the Halcon metamorphics. The alluvial gold is be-

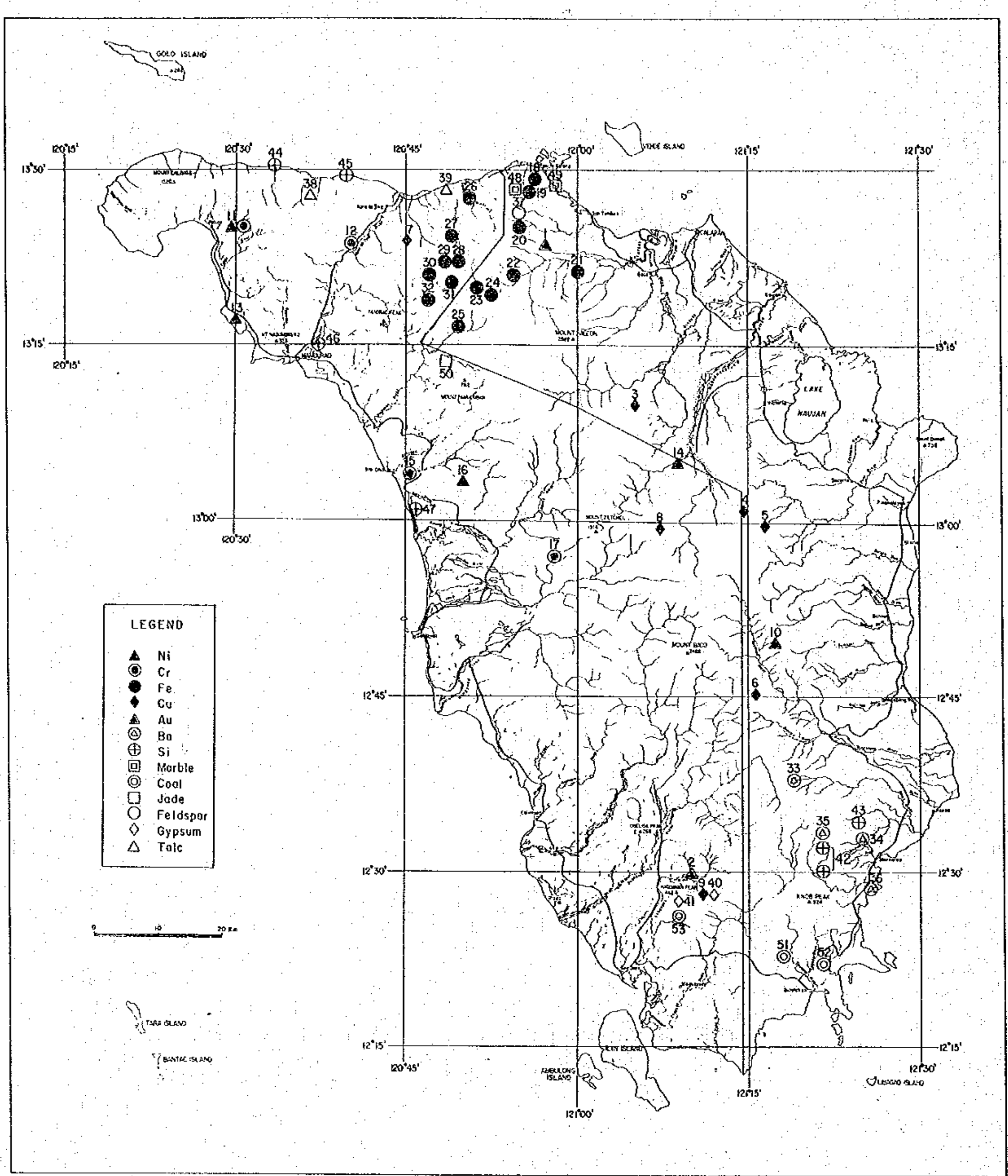

Fig. I-11 Location Map of Mineral Showings

ing collected by pouring the course grains of river sand through wooden boxes called sluice boxes. In some locations, such as the Agbuyt River at Saclag, the coarse sand is gathered by digging an adit in the river bed on both banks.

The alluvial gold samples come in a range of sizes. Many of them are rounded from 0.5 to 1mm in size. Sometimes massive samples are found while some samples are scaly. Recently large samples of alluvial gold exceeding 40g were found in the Agbuyt River.

There is no information as to the origin of this alluvial gold, but because igneous rocks are rarely observed in this area. It is presumed that these gold comes from metamorphic rocks. An analysis was performed on the quartz veins which exist along the schistosity of the metamorphic rocks of the Binaybay area, and on the clear and opaque quartz veins which cut through these, but no evidence of silver or gold could be found.

(B) The western area

The alluvial gold of the western part of the area is mainly collected from the Labangan River about 20km NNE of San Jose. The sluice box is not used here and panning is the usual procedure employed.

In this neighborhood the drainage system is composed of Pliocene conglomerate of the Bongabong group, which uncomformably covers the Sablayan group which is comprised mostly of Eocene-Oligocene limestone. The fact that alluvial gold is abundant in the area where conglomerate formations are found has been determined from experience.

As explained above, the alluvial gold deposits in Mindoro Island are limited in their area of distribution.

2–2–2 Copper ore deposits

Earlier reports of copper ore deposits dealt with 5 places in the area of the Mindoro fault, 2 places in the northern parts, and 1 place in the south. All are considered to be related to the acidic igneous rock.

(A) San Andres ore deposit

This ore deposit is in the upper reaches of the Bukayao River, and is located approximately 10 km northwest of Villacervesa. The geology is composed of quartz-sericite schists of the Halcon metamorphics, nearby to the east runs the Mindoro fault. Ultramafic rocks which consist of serpentine-dunite-pyroxenite found along the Mindoro fault (BM 1974), can be seen.

The ore deposits are chalcopyrite-pyrite-quartz veins which are found in the quartz-sericite schists, the outcrops of which are scattered around over a length of about 3.5km in a

NW–SE direction. The vein ordinarily runs along the schist, but there are also times when it cuts across the schist.

An ore vein from three main outcrops was reported as being from 0.5 to 2.0m thick, with the grade of Cu between 0.95–9.92%, but the results of the chemical analysis on samples gathered from the outcrops in the southernmost parts of this survey are as follows.

Chemical analysis:

Sample no.	width	Au g/t	Au g/t	Cu %	Fe %	S %
WR–183	0.10m	0.0	1.3	0.37	7.63	1.80
WR–185	0.10m	0.0	0.9	0.15	18.52	6.60

Under the microscope both samples show small amounts of chalcopyrite, colloform pyrite, and sphalerite in the quartz veins.

(B) The Acliang and Pajo ore deposits

These ore deposits are located in the Acliang and Pajo creeks, a western tributary of the Bongabong River, and are found in the sericite-chlorite-amphibole schists of the Halcon metamorphics.

Ore minerals are mostly pyrrhotite, accompanied by small amounts of chalcopyrite and pyrite. According to some existing data, the ore deposits are of vein-type formed along the schistosity, but could not ascertain the truth of this at this time. As for igneous rocks, there are the ultramafic rocks which run along approximately 10 km of the Mindoro fault in the eastern part, as well as the diorite which crops out on the banks of the Bongabong River for 10km in the southeast part. The latter (diorite) may be related to some mineralization.

Under the microscope, boulder float ores show a coarse or irregularly tabular chalcopyrite associated in the outer portions of the xenomorphic granular iron ore deposits. Colloform chalcopyrite of 0.5mm size, and coarse-grained sphalerite can be observed in small quantities.

The grade analysis of the same boulders are as follows.

Sample no.	Size	Au g/t	Ag g/t	Cu %	Fe %	S %
WR–142	5x5x10cm	0.0	2.2	0.69	37.70	29.81

According to this survey, at the southern bank of the Siange River 10km southeast of the above mineralization area, several centimeter wide pyrite-quartz veins in the sandstone of the Mansalay formation were found, and wall rock alteration (silicification) was quite widespread. These mineralized areas should be included phase II geological survey.

The chemical analysis of silicified zones are as follows:

Sample No.	width	Au g/t	Ag g/t	Cu %	Fe %	S %
WR--130	0.10m	2.9	3.4	0.0	21.26	19.90

(C) The Socorro mineralization zone

In the upper reaches of the Pula River about 25km west of Pinamalayan, there are two mineralization zones which have been prospected by the Zion Exploration Corp. and the Mindoro Mining Corp. They are within 5km from each other, and on the same mineralization.

This neighborhood is a region where ultramafic rocks intruded into the Mansalay formation along the Mindoro fault are found. The northern and eastern sides of this rock group is unconformably underlain by sedimentary rocks of middle to late Tertiary Period.

The zone of mineralization, according to the record (BM 1974), is a metalliferous vein which fills up the fissure of the fault or the sheared zone of the ultramafic rocks of the Mansalay formation, and is formed by massive sulfide deposits or quartz lenses. Ore minerals include chalcopyrite, pyrite and pyrrhotite, and appear to be impregnated in the quartz lens. There is a report indicating that in the region of the Zion Exploration Group the width of the massive ores are from 10 to 30cm, and of the quartz lenses from 30 to 50cm.

(D) The Balao mineralization zone

This mineralization zone is in an eastern tributary of Abra de Ilog River, and a publication has reported nine outcrops in the area. The geology of this area is composed of amphibolite and quartz schists which are intruded by diorite. The mineralization zone is in the massive amphibole-pyroxene-garnet hornfels which develops along the area directly connected to the shear-zone and diorite (BM 1974). Pyrite and very small amounts of chalcopyrite can be seen.

The grades of each outcrop are from 0 to 0.093% Cu and 0 to 1.08 g/t Au, which are extremely low grades.

2–2–3 Nickel-chrome ore deposits

The nickel-chrome ore deposits in Minodoro Island are found along the western shores and along the Mindoro fault, and are related to the ultramafic rocks.

There are no mines in operation at present, but the main ones which were explored before are as follows.

(A) Aglubang nickel ore deposits

This ore deposit is on the western bank in the upper reaches of the Magasawangtubig

River and is located in the eastern Mindoro and western Mindoro provinces. The claim areas of both regions are complicated, and survey reports concerning both have been compiled. Because both are considered to be the same ore deposit, it was given the tentative name Aglubang ore deposit, from the name of the village.

The geology of this neighborhood consists of gabbro and peridotite (dunite) which intrude into sericite-chlorite-amphibole schists of the Halcon metamorphic rock groups. In the places where these intrusive rocks are found, the entire mountain slope is weathering into red-yellowish laterite.

The ore deposits are nickeliferous laterite deposits, but in the past the Anglo Philippine Oil Corp. carried out an auger exploration in the area. According to this survey, it was calculated that the thickness of the laterite was from 3 to 11m (average 5m), with ore reserves of 49,000,000T, and a grade of about 0.94% Ni.

In this survey after analyzing the laterite obtained from the place which appeared to be a trench site, the following results were obtained.

Chemical analysis:

Sample No.	Cr %	Ni %	Mg %	Fe %	Al %
WR–160	2.65	0.46	2.15	28.70	3.79

(B) The Paluan chrome deposits

This ore deposit is located on the flank of the southern bank of the Muriel River about 4km southeast of Paluan. From the area between the provincial roads of Mamburao and Paluan it takes about 30 minutes on foot.

The geology consists of serpentine which intrudes the mica schists of Halcon metamorphics, and here the width of the dikes are about 500m. The chromite deposits in serpentine in some area are being explored by stripping or trenching. It has been reported that there were mining operations taking place here, but now there is only one place where low grade lenticular ores (size 0.2 x 0.5 x 1.0m) are found in the serpentine, and small amounts (size 0.10m) of chrome ore in the stockpiles can be observed.

The grade analysis of each of the above are as follows.

Sample No.	Cr %	Ni %	Mg %	Fe %	Al %
FR–07 (stockpile)	30.71	0.07	6.44	4.59	2.16
FR–08 (outcrop)	0.02	0.02	9.65	0.44	6.42

Under the microscope sample (FR–07) is seen to be composed of aggregates of chromite

of size 0.5mm, but one part was fragmented (size 0.05mm). A cataclastic texture can be seen. This indicates that the chromite was fragmented at the same period as the intrusive period of serpentine.

According to the BMG report (1974), nickeliferous laterite with an average width of 1m is found in this area, and a 0.24% Ni grade analysis was obtained.

(C) Other ore deposits

In the upper reaches of the Bongabong River, the Blueridge Mining Corp. found nickeliferous laterite ore deposits. Geochemical analysis of samples of 0.80–2.95%Ni have been reported. Because of peace problems, however, the survey was suspended.

In the western parts of Mindoro Island, the Igsoso nickeliferous laterite ore deposits and the Sta. Cruz chrome ore deposits have been reported, but since the reports are old, their locations are unclear. The ultramafic rocks which crops out in the lower reaches of the Amnay River had been explored during the chrome boom as shown by numerous miners' test pits. But now they buried, and the stockpile cannot even be found. The grade analysis of soil taken from 2 places which were thought to be old test pits are shown as follows:

Grade analysis:

Sample No.	Cr %	Ni %	Mg %	Fe %	Al %
SR–39	0.26	0.22	26.20	5.43	0.43
SR-60	0.26	0.21	23.16	5.43	0.68

2–2–4 Iron ore deposits

Near the summit of the northern part of the central mountain range, many iron ore deposits are known to exist, and there are also areas where drilling or tunneling have taken place. The ore deposits are thought to be metasomatic deposits, and originate in the limestone which unconformably covers the metamorphic rocks or the Halcon metamorphics.

The main iron ore deposits are as follows.

(A) The Lasala and Nagsabongan ore deposits

Both of these ore deposits are located in the upper reaches of the Mamburao River, and are in the Eocene limestone which unconformably covers the Halcon metamorphics.

According to existing records, the Lasala ore deposits are on the western banks of the Mamburao River, and during the period 1961–1964, prospecting was carried out by the Mayorga Mining Co. The first ore body was discovered beneath the river bed by a dip needle survey. After that, systematic drilling on the western flank where outcrops were discovered

was carried out, and a large amount of ore was discovered.

The Nagsabongan ore deposits are in the upper reaches of the Lasala ore deposits, and are located on the northern bank of the Mamburao River. These ore deposits have also undergone magnetic survey, drilling, trenching and tunneling during the period 1962–1964, by the Mayorga Mining Co. The results showed a width of 92 x 65m. An iron ore deposit (Fe of over 60%) having a thickness of 35m in the central part was discovered.

These ore deposits in were not examined in this survey, but in the river beds of the area where these ore deposits are found there are countless scattered boulders, some of which have a diameter of over 100cm.

These boulders are made up of large amounts of hemadite, epidote and garnet, and under the microscope, show that magnetite is partly altered by lattice structured acicular hematite.

Grade analysis of representative samples:

Sample No.	Size	Fe %	S %	Si %	Al %	P %
FR–31	30x30x20cm	54.13	0.20	1.14	0.13	0.00

The occurrence of the ore deposits could not examined but because both deposits are accompanied by skarn minerals and exist in limestone, it is considered to be contact metasomatic.

(B) The Dayap ore deposits

This ore deposit is in the upper reaches of the Pagbahan River, about 90km from the mouth, and is found in the limestone which is part of the Mansalay formation.

According to existing data, this ore deposit is found to be concordant with schistosity or skarn schistosity, and generally becomes platy, but pockets and veins are also seen. The following three outcrops are known.

No. 1. Two exposures separated by 50m and each having widths of about 6m. Because of the location of the boulders which are found, both are considered to be of the same horizon.

No. 2. Having a width of 8m, one can follow the outcrop horizontally for 80m. The ores are made up of over 50% magnetite, including skarn minerals.

No. 3. This is the largest ore bed. There are five layers totalling about 70m wide (bed width approximately 15m) which consists of magnetite and skarn minerals, the strike direction can be followed for 40m. In the 45m zone below this ore bed up to the quartz diorite bodies, garnet-epidote is developed.

The microscopic characteristics and chemical analysis of the boulders which were obtain-

ed from the river bed are as follows.

Chemical analysis:

Sample No.	Size	Fe %	S %	Si %	Al %	P %
FR–45	20x10x10cm	50.48	0.24	6.57	0.42	0.00

Microscopic characteristics:

Sample FR–45 A large portion is magnetite, with small amounts of acicular hematite arranged in a lattice structure. Also small traces of chalcopyrite (diameter less than 0.1mm) with sphalerite surrounding it were recognized.

(C) The Binaybay mineralization zone

This mineralization is a small part of the mountain summit on the southern bank of the middle reaches of the Alag River. This area is composed of gneiss, amphibolite, recrystalline limestone and mica schists which exist in the Halcon metamorphic rocks. The iron ore deposits are found as big boulder groups, with a diameter of 1.5m within the 15 x 15m area of the limestone zone. It was discovered by test pitting that these extended downward.

The ore minerals are considered to be mostly hematite, with small amounts of magnetite.

Boulders of these ores were not investigated but they are also considered to probably be a contact metasomatic deposit.

2–2–5 Barite ore deposits

The barite ore deposits of Mindoro Island are located in the southern part of eastern Mindoro, and exists as a metalliferous vein in the Mansalay formation. At present there is only one mine in operation, but two other ore deposit areas are known.

The details of the ore deposit based on the survey are as follows.

(A) The Taoga ore deposits

This ore deposit is located 18km northwest of Mansalay, and is found on the bank of the upper reaches of the Baroc River, 700m above sea level. A truck road of 30km length runs along the ridge from Mansalay to the mine site.

This ore deposit was developed and produced by the Frontino Inc. but was closed in 1974.

In January 1982 it was re-opened by Filhispano Inc. and at present there are 15 people employed in mining operations there. In the initial period from January to March, 600 tons of ore were mined, and of this 200 tons have been consigned.

This area consists alternating layers of thick sandstone and shale which are found in the

lower section of the Mansalay formation. These ore deposits are in the form of veins which fill the fractures in the sandstone, having a width of 10m, as shown by no. 1 and no. 2 veins as the main veins. (Fig. I–12).

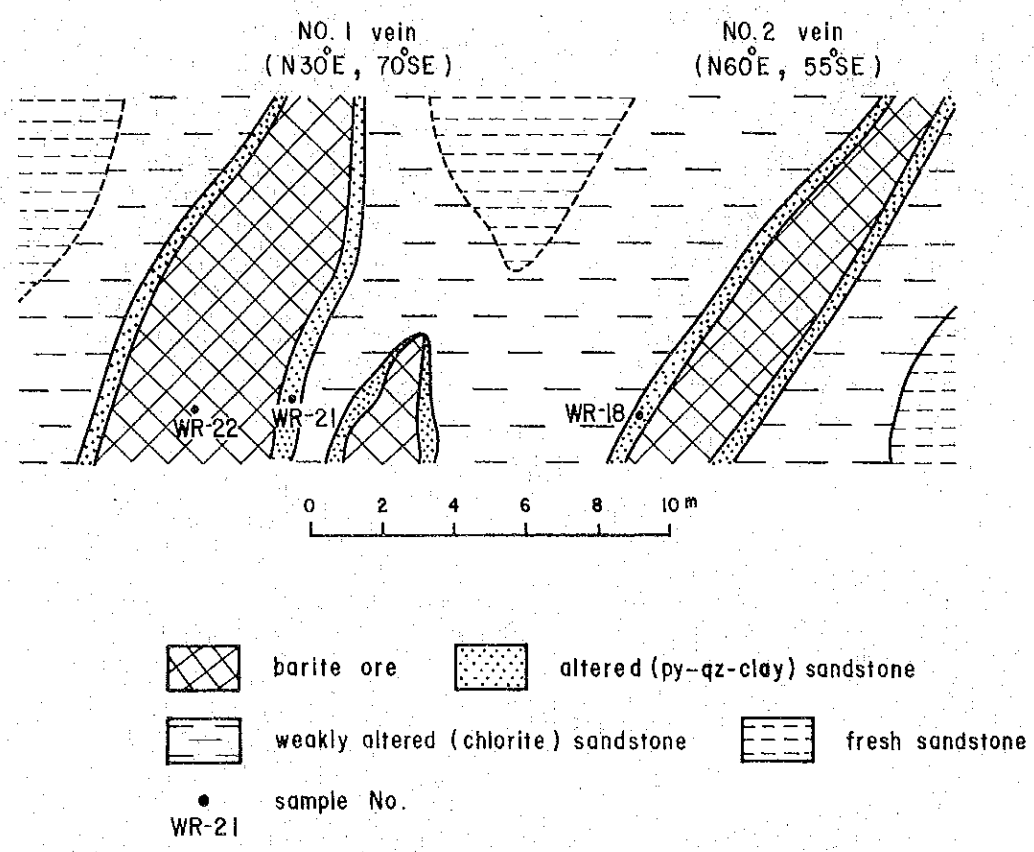

Fig. I–12 Sketch showing Barite Veins, Taoga Deposits

The no. 1 veins has a strike of N30E, dipping 70S, and the vein width is about 5m (reaching 10m at its longest, in some parts), a strike length of over 20m, and a dip elongation of over 20m. According to recent strip production, the vein width decreases abruptly towards the lower levels, and thus the entire ore body is assumed to be lenticular.

The No. 2 vein is an ore body where strip production has ended and mining has just begun, and shows a strike direction of N60E and a dip of 55S. The average vein width is 2.5m, the strike length is over 10m, and the dip elongation is over 10m.

Towards the upper portion there is a tendency for the vein width to pinch out.

Fig. I--13 No. 2 Barite Vein, Taoga Deposits

Both the No. 1 vein and No. 2 vein are massive white ores formed by barite crystal aggregates ranging in size from a few millimeters to a few centimeters, and include very small amounts of pyrite locally. Gangue minerals can rarely be seen.

According to X ray analysis, mica, barite, quartz, pyrite, sericite, and montmorillonite have been detected in the host rock adjascent to the veins. The host rock, a few meters from the veins is chloritized.

The analyses of the altered rocks near the vein and the ores gave the following results.

Sample No.	Width	$BaSO_4$ %	SiO_2 %	Fe_2O_3 %	CaO %	Al_2O_3 %
WR--22 (No.1 vein)	2.00m	83.79	2.55	0.17	0.01	0.00
		Au g/t	Ag g/t	Cu %	Fe %	S %
WR--21 (No.1 wall rock)	0.30m	1.5	2.5	0.00	10.55	10.54
WR--18 (No.2 wall rock)	0.20m	0.2	1.3	0.00	8,95	10.84

(B) The ore showings of Mansiol point

This ore showings is on the hill (60m above sea level) 1.3km west of Mansiol point in the southern part of Mansalay. This area is composed of sandstone-mudstone alternating layers of the Mansalay formation. Barite was observed as boulders of middle to large sized floats, continuously for over 20m along a S25E direction.

There are no records of previous mining or prospecting in this area. Based on the physical

features, mode of occurrence and quantity could easily be proven by trenching.

2–2–6 Silica sand deposit

The silica sand deposit in this island can be divided into two groups. One, where quartz was derived from basement rock and is found on the northwestern shores, and the other is the arkose sandstone of the Mansalay formation.

(A) Maria Cristina deposits

This deposit is found on the shore 8km northwest of Abra de Ilog. The sub-rounded to rounded pebbles of quartz are 1.5km in length, and a width of 0.3m, they are concentrated in an area with an average width of 20m.

According to some existing data, quartz makes up an average of 20% of all rocks. The confirmed ore quantities of 3600 tons, with grades of 80–97% SiO_2, 1.21% Al_2O_3, 0.32% FeO and 0.37% CaO.

(B) The deposits of Falcon Mineral, Inc.

This deposit is located on a flat part 150m above sea level, 3km northwest of Mansalay, and is made up of the arkose sandstone of the Mansalay formation. In the mining area which was until recently in operation, white to light grey in color, coarse-grained, massive rocks of over 20m in thickness were mined, and five bench levels had been established.

Fig. I–14 Silica Quarry, Falcon Mineral Inc.

Under the microscope, this sandstone was found to consist mainly of quartz, K-feldspar, and plagioclase, and included small amounts of other rock fragments such as slate and chert.

This arkose sandstone bed outcrops in numerous places, even on the forest roads which lead to the aforementioned Taoga barite deposits, and is also established in some claims of the silica sand deposits.

Near the shore of the northeastern parts of the Mansalay town, are found about 100 tons of silica sand stockpile which are thought to have been mined in this area. The grade quality is as follows.

Sample No.	SiO_2 %	Al_2O_3 %	K_2O %	Na_2O %	FeO %
WR−17	82.40	4.95	3.06	0.47	0.58

2−2−7 Marble deposits

The marble deposits are in the area of Puerto Galera in the north, and are scattered in the Halcon metamorphics. It seems that small scale mining was previously carried out in each of the areas, but at the present only the Dulangan deposit near the provincial road is in operation. This deposit produces 2 m^3/day of fine-grained white marble intercalated in the mica schist, and is consigned in Manila. The deposit is thought to have a strike elongation of 800m, a width of 150m, and height of about 50m. According to some provincial data (1981), deposit reserves are assumed to be 110,070,000 tons.

2−2−8 Coal deposits

The coal deposits found in this island are limited to the southern areas. They are located in the Napisian region of northern Bulalacao, the Siay region, and the Alitaytayan region of eastern San Jose.

These deposits are found in the Sabulayan formation, and in the alternating layers of sandstone-mudstone of the lower levels of the same formation. In San Jose they are scattered in the sandstone intercalated in the thick limestone.

The characteristics of the deposits are given below.

(A) Bulalacao area

The coal deposit of this area has been known for 100 years, and the development of this area had been planned many times, but a proper level of production was never reached. From

November 1952 to March 1953 the BMG established the geological stratigraphy of this area, and with the purpose of estimating the coal reserves, carried out a survey with the advice and aid of the USGS, and reported on those (good) results (1955). Recently the Construction and Development Corp. of the Philippines (CDCP) has been carrying out a systematic drilling exploration program in the Napisian region, leading up to the present time.

A–1 The Napisian region

This region is located 7km northwest of Bulalacao, and many coal seams are exposed along the Napisian river which flows south through the central part of the region.

The geology of this region is made up of the Napisian formation, comprised primarily of clastic rocks and the Mato-ang limestone formation, according to Weller & Vergara (1955). Also, the region includes the present Sabulayan formation. The layer width is assumed to be about 100m in the upper Mato-ang formation, and 450m in the lower Napisian formation.

The coal bearing formation is located in the upper parts of the Napisian formation, and is composed of impure limestone, unsorted clastic rocks, and at least 10 layers. Of these, the clastic rocks are composed mainly of silt and shale, and include sandstone and conglomerates. The limestone appears as a lens under 1m thick, and many layers are observed in the neighborhood of the coal deposits.

The coal formation has a thickness of less than 3m, and according to some existing data (Weller J.M. et al. 1955), it is intercalated with brown, dark grey, or black shale. However, according to observations on the outcrops and core samples, the coal formations were seen in abundance in the fine to midium-grained sandstone (Fig. I–15, 16)

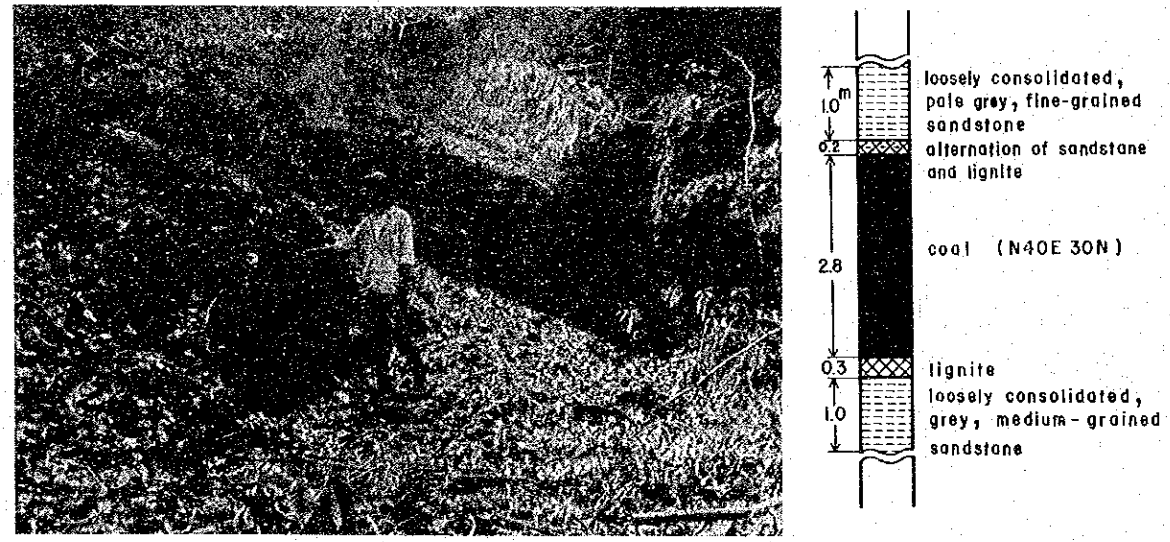

Fig. I–15 Outcrop of Coal Seam, Napisian Area

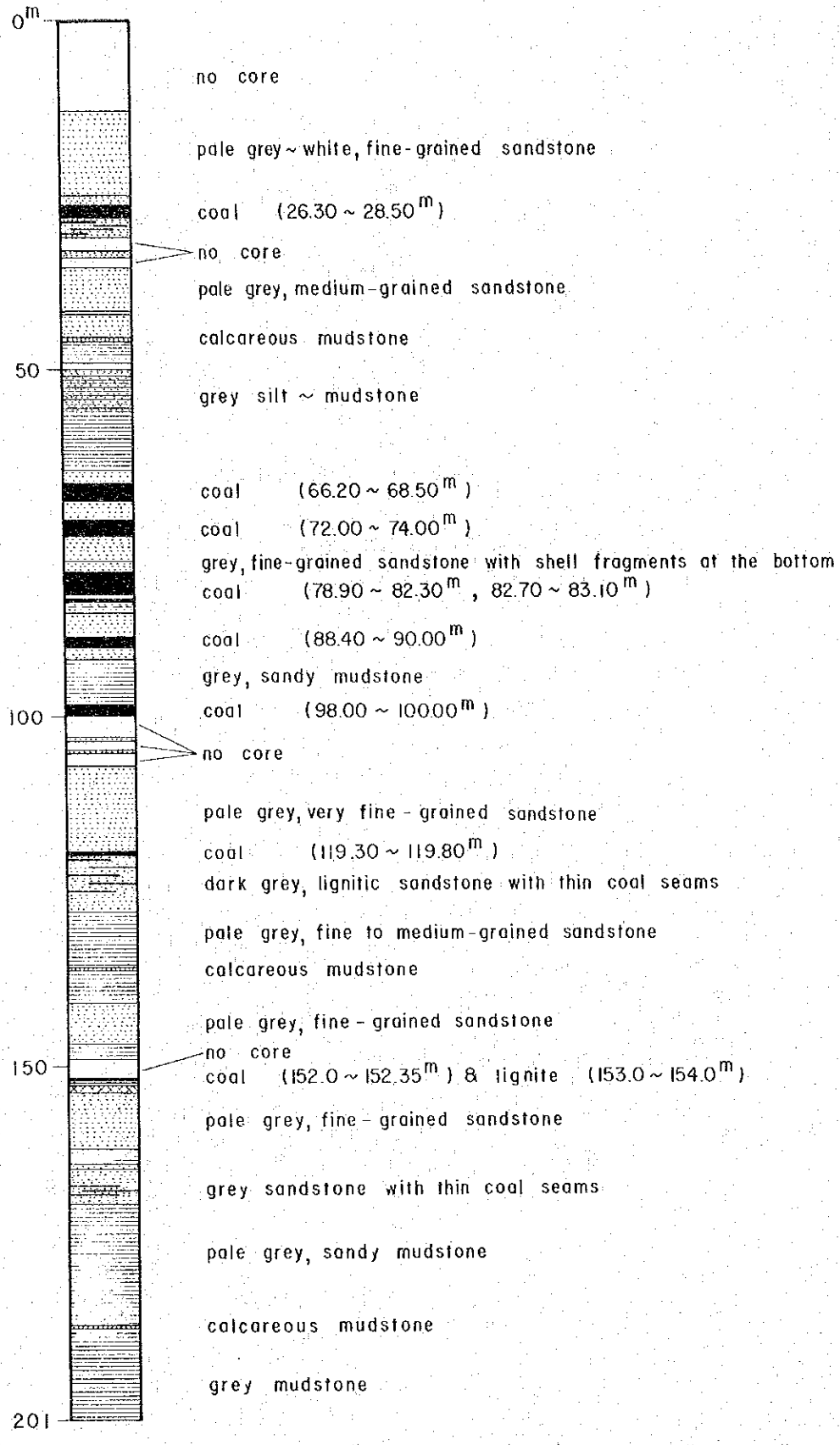

Fig. I-16 Core Log of DDH NP3-1, Napisian

The coal formation of this region consist of at least 10 seams. It was reported that the four seams from which coal was produced were over 0.75m thick. However, as shown in Fig. I–16, 10 layers, including layers of lignitic coal, were found by core drilling, and of these 6 were over 0.75m thick, with the thickest being 3m.

The coal reserves, according to the BMG report (Weller J.M. et al. 1955) are given in the next table:

Table I–5 Coal Reserves of the Napisian Area

Thick Coal (75 cm. or more)

Level	Measured	Indicated	Inferred	Total
Above drainage		194,000	389,000	583,000
Drainage to –200 m.	672,000		3,831,000	4,503,000
Total	672,000	194,000	4,220,000	5,086,000

Thin Coal (35 to 75 cm.)

Level	Measured	Indicated	Inferred	Total
Above drainage			200,000	200,000
Drainage to –200 m.	214,000		1,276,000	1,490,000
Total	214,000		1,476,000	1,690,000

Total estimated coal in Napisian area – 6,776,000 metric tons.

The result of analysis is as follows:

	water content	volatile component	inert content	ash content	calorific value
Average of 8 samples	27.7%	37.1%	31%	3.7%	12,023BTU/lb

This calorific value is consistent with the high volatility "C" bituminous coal, as reported by the American coal standard (ASIM, 1964).

A–2 The Siay region

This region is located 5km northeast of Bulalacao, and 6.5km east of the Napisian region.

The geology of this region is made up of the Pocanil formation, which is the upper part of the Sablayan group (Corby et al., 1931). This formation consists mainly of shales, silts, and sandstones, but 35m of limestone are included.

The coal seams are located in the shale at the center of the Pocanil formation, and have a thickness of between 0.10 and 1.20m. In the limestone formation, 7 coal seams can be seen. There are three coal seams with thicknesses of 0.75m from which coal is produced, and according to the BMG, the coal reserves are as follows:

Table I–6 Coal Reserves of the Siay Area

Thick Coal (75 cm. or more)

Level	Measured	Indicated	Inferred	Total
Above drainage	7,000			7,000
Drainage to −200 m.	58,000	109,000	136,000	303,000
Total	65,000	109,000	136,000	310,000

Thin Coal (35 to 75 cm.)

Level	Measured	Indicated	Inferred	Total
Above drainage	3,000			3,000
Drainage to −200 m.	25,000	66,000	56,000	147,000
Total	28,000	66,000	56,000	150,000

Total estimated coal in Siay area – 460,000 metric tons.

The result of analysis is as follows:

	water content	volatile component	inert component	ash component	calorific value
1 sample	5.8%	45.4%	45.6%	3.2%	11,850BTU/lb

By the American coal standard (ASIM, 1964), this qualifies as high-volatility "C" bituminous coal.

(B) The Alitaytayan region

This area is located in a region about 13km northeast of San Jose, and like the Bulalacao area mentioned above, is composed of interlayered sandstone and shale, and also from the thick limestone of the Sablayan group.

The coal can be seen in two layers in the sandstone and shale, and of these, the upper coal seam is 0.60m thick, with a short strike elongation, while the lower coal seam is 1.05m thick, and appears to have a strike elongation greater than 18m.

The outcrops which were investigated at this time are shown in Fig. I–17.

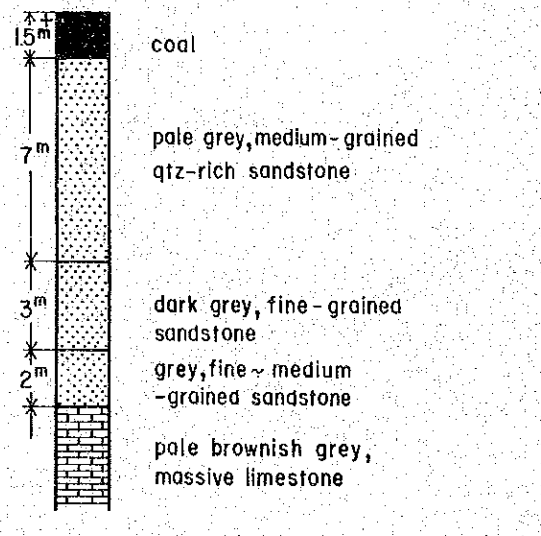

Fig. I–17 Outcrop of Coal Seam, Aritaytayan Area

Here is a grey to dark-grey in color, fine to midium-grained sandstone of about 1m thickness over the massive, thick limestone. The coal formation lies on top of this. Due to the lack of outcrops, the extent of the coal formation could not be determined.

The results of the sample analyses from this area are as follows:

water content	volatile component	inert component	ash content	calorific value	total sulph	viscosity
18.0%	39.4%	36.0%	6.6%	5.240cal/g	4.4%	0%

This calorific value having recalculated free water and ash contents in English units is 12,624 BTU/lb.

According to the American coal standard this is a high-volatile "C" bituminous coal.

Unfortunately there are no reports concerning the reserves in this area.

PART II GEOCHEMICAL SURVEY

Chapter 1 General Remarks

Based on the previous reports, the central mountain range in Mindoro is chiefly composed of basement rocks and ultramafic rocks in which mineral showings of copper, nickel and barite etc. are known. This zone is on the southern extension of basement and ultramafic zone of Zambales, Luzon. At the beginning of the survey the writers, therefore, expected not only nickel-chrome deposits of Zambales type but porphyry copper deposits of Dizon type which has been accompanied by quartz diorite rocks of Miocene.

The geochemical reconnaissance stream sediment survey of this phase was carried out together with the geological survey. The collected samples were analyzed for ten (10) elements of Cu, Ni, Cr, Pb, Zn, W, Ag, Fe, Mn and Mo in order to check adaptability of the geochemical survey. As the result, drainages with high Ni and Cr contents correspond to the ultramafics distribution and five geochemical anomalous zones were detected. One Cu-Zn and two Ag anomalous zones could be found but no Fe anomalies were obtained in the drainage where iron deposit with a scale of 1,000,000 ton can be expected (Table II–1).

From a viewpoint of the distribution of heavy minerals collected from almost all drainage systems, chromite concentration well corresponds to the distribution of ultramafic rocks.

Table Ⅱ-1 Summary of Geochemical Survey Results

Factor 1

Name of Anomalous Zone	Area (km^2)	Element	Ni			Cr			Geology	Mineralization
			No. of Anomalies		Max. Value (ppm)	No. of Anomalies		Max. Value (ppm)		
			1st	2nd		1st	2nd			
Paragpagan	8	Ni	2	1	900	1	0	1,448	Ultramafic rocks	Exploration for nickeliferous laterite had been carried out.
Amnay River	5	Ni–Cr	2	1	1,920	2	1	2,086	do	Unencountered
Villacervesa	94	Ni–Cr	4	1	1,722	2	2	6,466	do	Anglo Philippine Oil Corp. explored nickeliferous laterite. Reserve: 49MT(0.94 Ni)
Pula River	3	Cr	3	0	868	3	2	10,565	Fine tuff. (Bongabong G.)	Unencountered
Bansud River	62	Ni–Cr	10	9	2,288	6	4	2,976	Ultramafic rocks	Blueridge Mining Corp. explored nickeliferous laterite in this zone

Factor 2

Name of Anomalous Zone	Area (km^2)	Element	Cu		Zn		Geology	Mineralization
			No. of Anomalies	Max. Value (ppm)	No. of Anomalies	Max. Value (ppm)		
			1st		1st			
Rayusan	76	Zn	1	158	5	204	Slate (Mansalay F.) & basalt (Lumintao F.)	Unencountered
Siange River	52	Cu–Zn	3	451	7	520	Sandstone (Mansalay F.)	A few pyrite-quartz veinlets

Factor 3

Name of Anomalous Zone	Area (km^2)	Element	Ag		Geology	Mineralization
			No. of Anomalies	Max. Value (ppm)		
			1st			
Alitaytayan	12	Ag	3	3.2	Limestone (Sablayan G.)	Unencountered
Mongpong	22	Ag	4	2.3	do	do

Chapter 2 Geochemical Stream Sediment Survey

2–1 Sampling

Generally silty sediments (under 80-mesh fraction) deposited in the active channels of streams were collected for geochemical samples. Care was taken to avoid mud and organic materials when sampling. As the geological survey was carried out along the main rivers, sampling were concentrated on their branches. In order to get more information from wider area, therefore, additional samples were collected from riverbeds at the foot of mountains.

About 20 grams of sediments were sampled and placed in vinyle bags after drainning off water. These were sent to the base camp for drying.

2–2 Analytical Method

All samples prepared at the base camp were sent to Japan. Eight (8) elements of Cu, Ni, Cr, Pb, Zn, Ag, Fe and Mn were analyzed quantitatively by atomic-absorption spectrophotometry and two (2) elements of W and Mo, by colorimetry.

2–3 Compilation and Interpretation of the Results

A histogram for each element was made from analytical data and then geochemical anomalous zones were extracted by multivariate analysis and unitary element analysis.

2–3–1 Histogram

All analytical data were transformed to logarithmical figures and divided into 20 classes in which maximum and minimum values are both end values of classes for making a histogram for each element (Fig. II–1 A, B). As the contents of Ag, W and Mo are such low that the numbers of lower values than detectable limits are 60%, 85% and 92% respectively, 0.0 ppm of Ag, 0.000% of W and 1 ppm of Mo were read as 0.01 ppm, 0.0001% and 0.1 ppm respectively. Histogram making and statistical treatment were carried out on these data.

The Histogram of each element approximates to normal distribution except 3 elements of Ag, W and Mo. Cr-histogram shows something like χ^2 distribution.

2–3–2 Multivariate Analysis

To extract a fewer representative and hypothetic factors which express variables among many analytical data (4,220pcs), factor analysis (varimax method) was applied. Cluster analy-

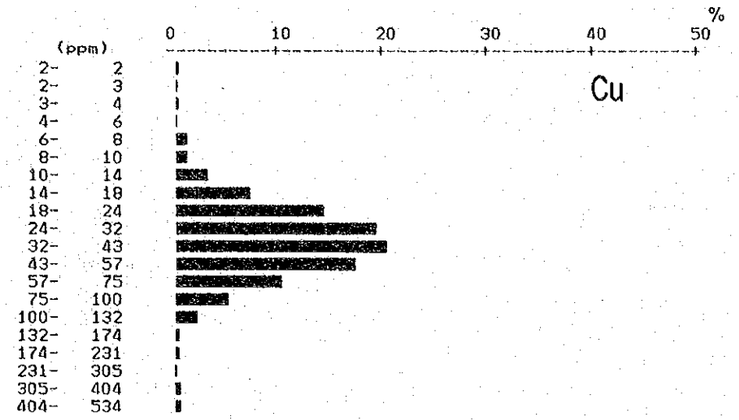

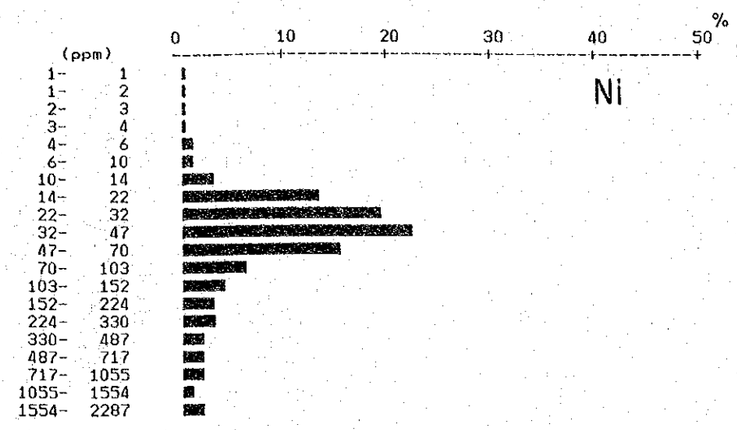

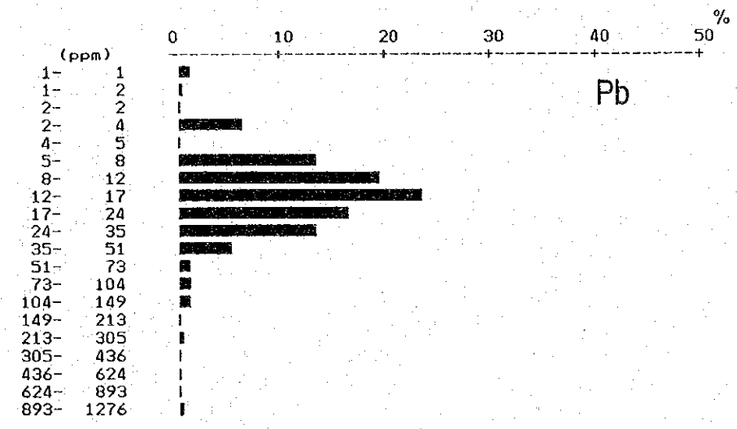

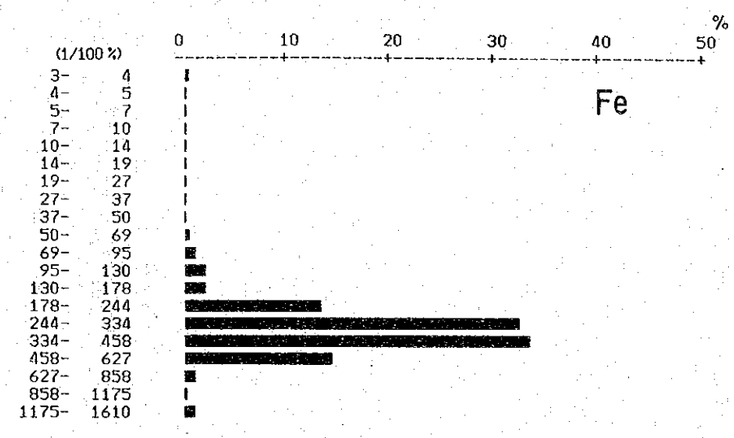

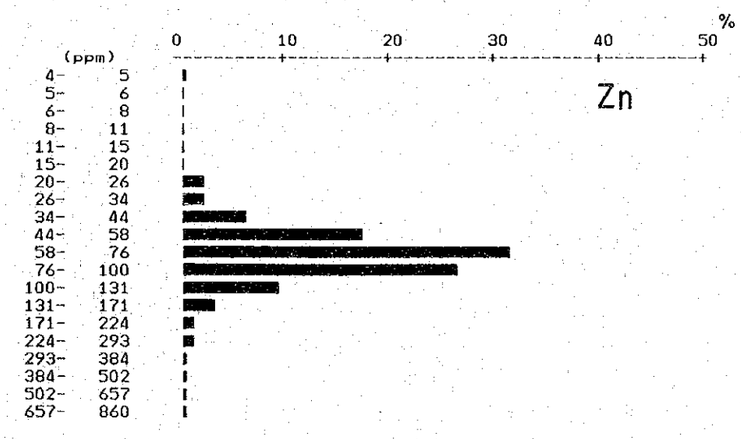

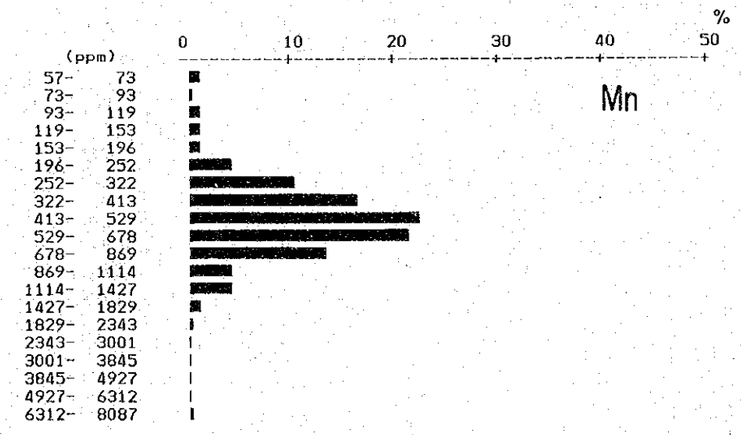

Fig. Ⅱ-1 A Histogram of Geochemical Data(Stream Sediment)

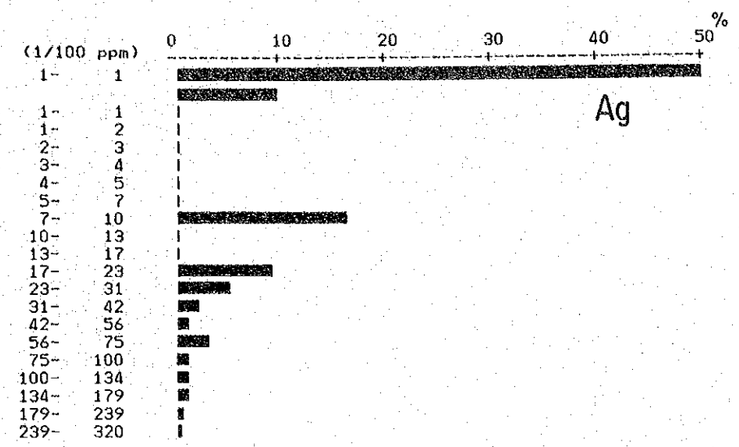

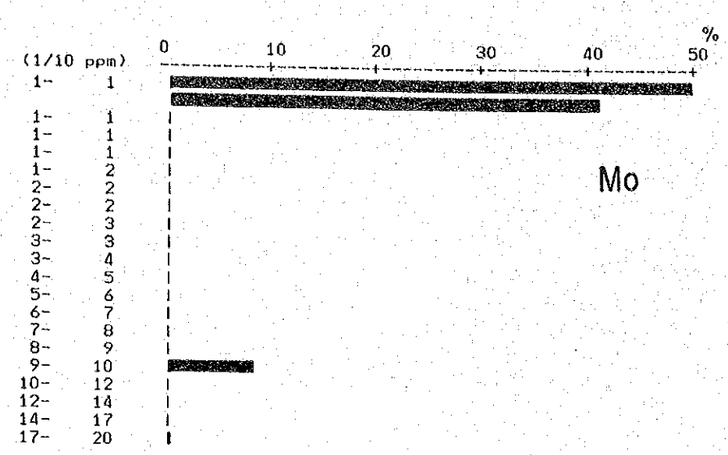

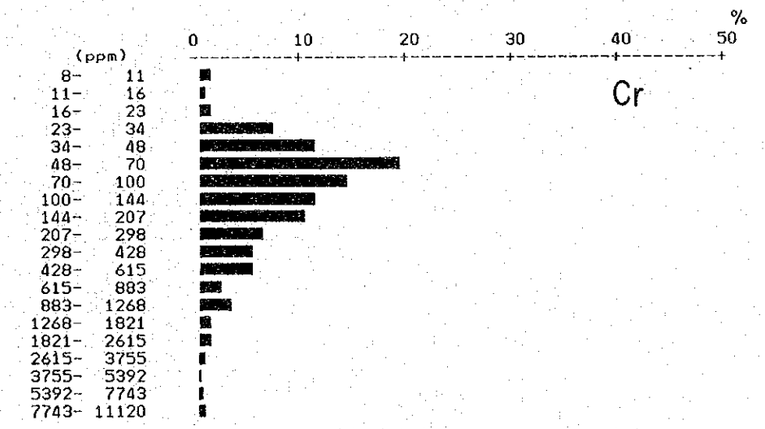

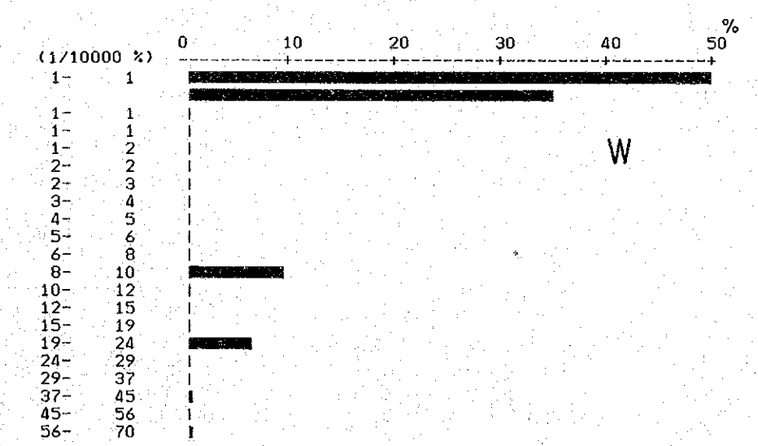

Fig. Ⅱ-1 B Histogram of Geochemical Data(Stream Sediment)

sis is also used supplementaly to clarify mutual relations between each element. Fig. II–2 shows a flow chart of multivariate and unitary element analyses.

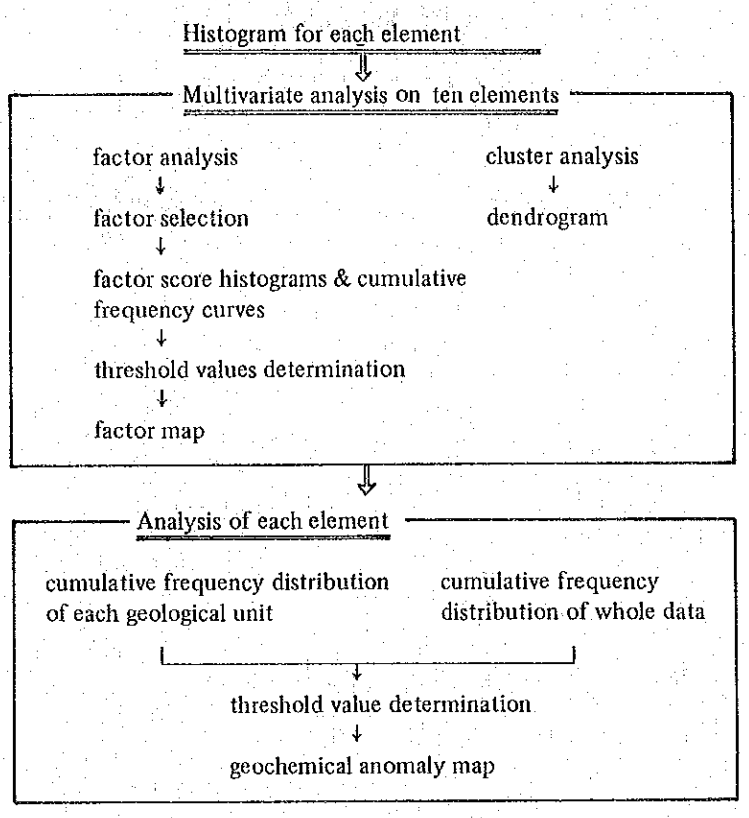

Fig. II–2 Flow Chart of Statistical Analysis

Extraction of anomalous values was based on both " a simplified statistical treatment of geochemical data by graphical representation (Lepeltier, 1964) " and some geological consideration.

The means and standard deviations by element are shown in Table II–2.

The correlation matrix between each element is shown in Table II–3. The four factors shown in Table II–4 were extracted by factor analysis with computer.

Table II–4 shows Factor 1 is characterized by Ni–Cr–(Fe)–(Mn) factor loadings and Factor 2, by Cu–Zn. In Factor 3, factor loadings of elements are not so high as in Factor 1 and 2, but Ag-loading is relatively high. In Factor 4, factor loadings of elements are too low to discuss.

Table II–2 Means and Standard Deviations of Geochemical Data

Element	Max. (ppm)	Min. (ppm)	Mean (ppm)	S.D. log	M+1xS.D. (ppm)	M+2xS.D. (ppm)
Cu	534	2	35.2	0.265	64.7	119.1
Pb	1276	0	14.4	0.346	31.9	70.9
Zn	560	4	70.1	0.200	111.2	145.0
Ni	2287	0	50.8	0.495	158.9	496.6
Fe	16.10(%)	0.03(%)	3.2(%)	0.205	5.1(%)	8.2(%)
Mn	8087	57	483.1	0.230	820.4	1393.2
Ag	3.2	0.0	–	–	–	–
Cr	11120	8	114.8	0.489	354.0	1091.4
W	0.007(%)	0.000(%)	–	–	–	–
Mo	2	< 1	–	–	–	–

M: Mean, S.D. : Standard Deviation

Table II–3 Correlation Matrix

	Cu	Pb	Zn	Ni	Fe	Mn	Ag	Cr	W	Mo
Cu										
Pb	0.161									
Zn	0.560	0.350								
Ni	0.116	–0.025	0.081							
Fe	0.415	0.138	0.399	0.500						
Mn	0.377	0.050	0.245	0.476	0.581					
Ag	0.037	0.155	–0.075	0.016	–0.011	0.093				
Cr	0.095	–0.178	0.015	0.856	0.542	0.493	–0.033			
W	–0.003	–0.034	–0.030	–0.053	0.004	0.015	–0.077	–0.047		
Mo	0.052	0.125	0.053	–0.101	0.010	0.032	0.141	–0.147	0.069	

Table II–4 Factor Loading of Geochemical Data

	Factor 1	Factor 2	Factor 3	Factor 4
Element	Factor Loading	Factor Loading	Factor Loading	Factor Loading
Cu	0.164	0.706	0.056	0.136
Pb	–0.108	0.357	0.326	–0.355
Zn	0.040	0.767	–0.018	–0.146
Ni	0.880	0.003	–0.093	–0.266
Fe	0.603	0.481	0.038	0.021
Mn	0.627	0.341	0.199	0.196
Ag	0.043	–0.048	0.417	–0.069
Cr	0.913	–0.045	–0.208	–0.064
W	–0.028	0.004	–0.000	0.175
Mo	–0.077	0.071	0.347	0.051

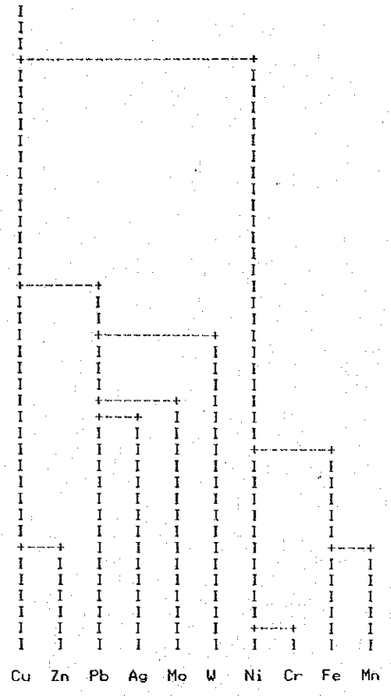

A. Dendrogram

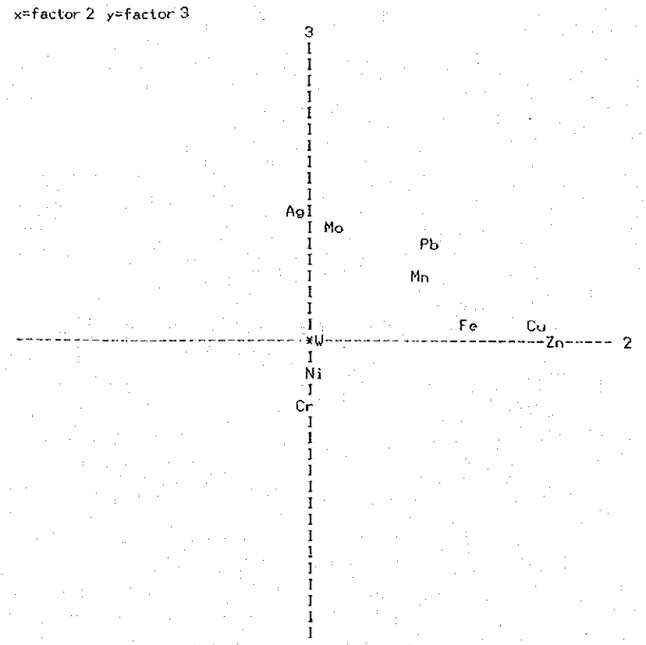

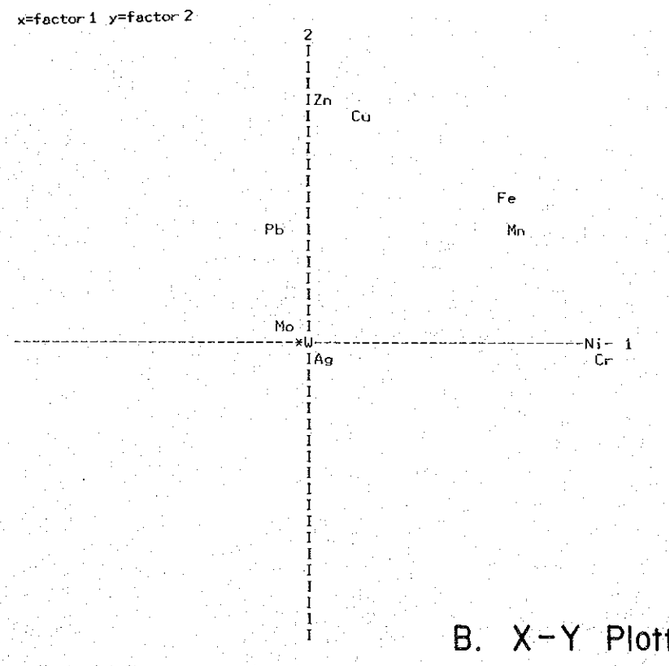

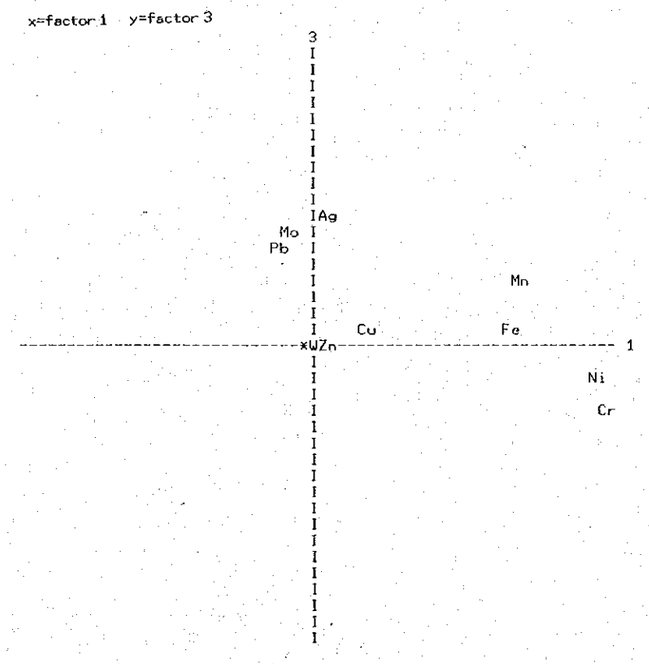

B. X-Y Plotting

Fig. Ⅱ-3 A·B Correlation Diagram.

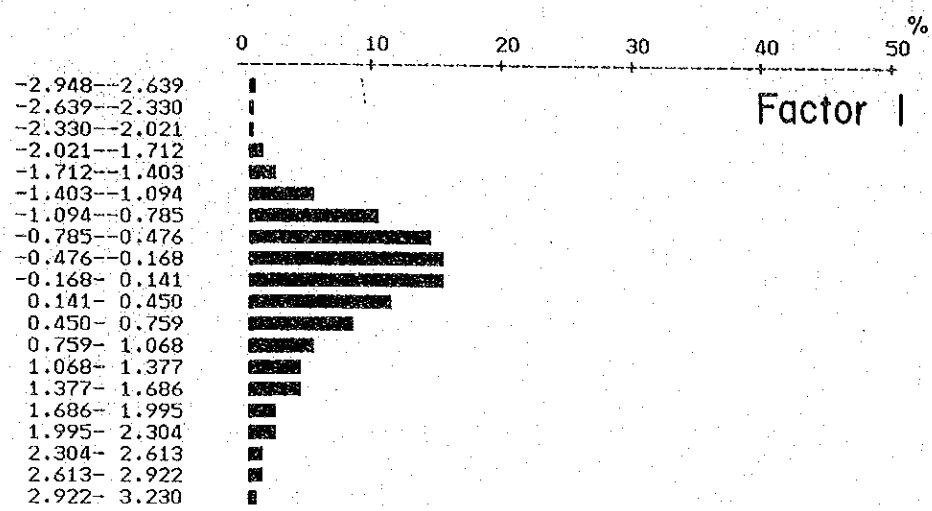

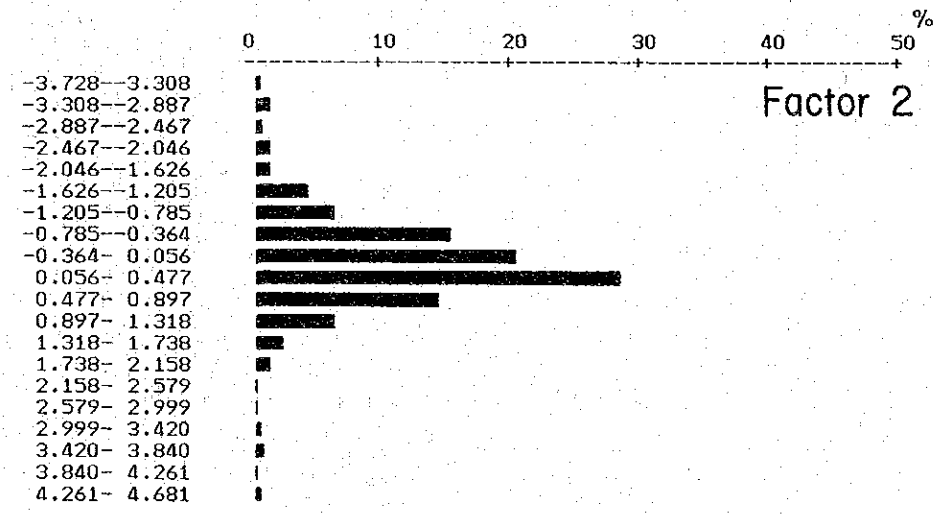

Fig. Ⅱ-4 Histogram of Factor Scores

To illustrate the correlation between each element, Fig. II–3 shows a dendrogram obtained by cluster analysis and X–Y plotting, by factor analysis. It is clear that Ni, Cr, Fe and Mn elements are closely connected with each other like Cu and Zn elements, indicating they have same trends of fluctuation.

Histograms of factor scores (Fig. II–4) and cumulative frequency distribution curves (Fig. II–5) were made for Factor 1 and 2 to construct a factor map from factor scores which were calculated by element.

The cumulative frequency distribution curve of Factor 1 has the breaking point at the abscissa of 25%. This breaking point is used to be taken as (t) if the break occurs above the normal threshold level of 2.5%. This time a homogeneous sampling pattern has not been obtained and the number of samples is not large enough to treat statistically by lithological unit, so that the mean + 2x standard deviation (M+2SD) has been taken as t instead of the 25% value. The same consideration was given for Factor 2. When only t is used for making a factor map, geochemical anomalies tend to be isolated, resulting in unclearness of the general trend of anomalies. Therefore, the values of t' = M + 1.5SD and t" = M+SD are used as supplement. The value of t"' = M + 2.5SD is also used to give an impression of very high value on the map.

The values of t, t', t" and t"' of Factor 1 and 2 are shown in Table II–5.

Table II–5 Regional Threshold Values of Factors

	t"	t'	t	t"'	Number of Anormalous Samples (pcs)	Number of Samples (pcs)
Factor 1	–	1.431	1.908	2.385	19	422
Factor 2	0.872	1.308	1.744	–	7	

t : Threshold value

Various methods can be considered to illustrate factor scores of stream sediments. In this report, the drainage basins were patterned with the kind of factors and the intensity of factor scores, on the basis of an idea that a factor score of stream sediment at the sampling sites is influenced by the whole basin. But when a drainage basin is very big, a patterned area was not whole basin but the limitted area near the sampling site. In this method, the geochemical anomalous zone is the sampled drainage basin itself. Therefore, the patterned anomalous zone has the advantage of showing directly the area to be checked. On the contrary, over- or under-

estimation of the anomalous zone may happen unless any consideration on the area of the basin is paid, because one sample represents whole of its basin.

Plate II–1–1 – 4 are factor maps thus obtained.

2–3–3 Unitary Element Analysis

As stated before, Factor 1 characterized by Ni–Cr–(Fe)–(Mn), Factor 2, by Cu–Zn and Factor 3, by Ag were extracted by factor analysis. Generally speaking, it is hard to consider that one kind of mineralization covers the whole survey area, so that a factor should be obtained when some mineralized samples are collected. On the assumption that there are no more factors indicating mineralization than the extracted factors, unitary element analysis was carried out for 5 elements of Ni, Cr, Cu, Zn and Ag which are closely related to the extracted factors.

Based on the geology of the sampled drainage basin, all samples can be divided into 7 geological units, viz. Socorro – Bongabong group, Sablayan group, Mamburao group, Lumintao formation, Mansalay formation, Halcon metamorphics and Ultramafics.

As shown in Table II–6, numbers of samples by geological unit are too small to get enough reliability for interpretation with a statistical method.

Table II-6 Number of Samples of Each Geological Unit

Geological Unit	Number of Samples (pcs)
Socorro G. & Bongabong G.	60
Sablayan G.	65
Mamburao G.	5
Lumintao F.	32
Mansalay F.	142
Halcon Metamorphics	85
Ultramafic rocks	33

To obtain the properties of the universe by geological unit, however, cumulative frequency distribution curves of Ni, Cr, Cu, Zn (Fig. II–6) were made for each geological unit except Mamburao group with very few samples.

As is obvious from the figure, Cu and Zn have relatively little differences in their contents by geological unit. There seem no problems to interprete analytical data collectively. But Ni

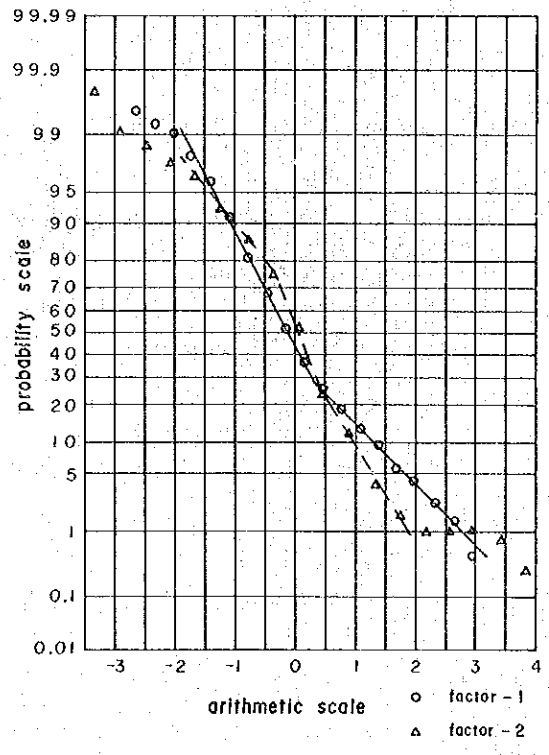

Fig. II–5 Cumulative Frequency Distribution of Factor Scores

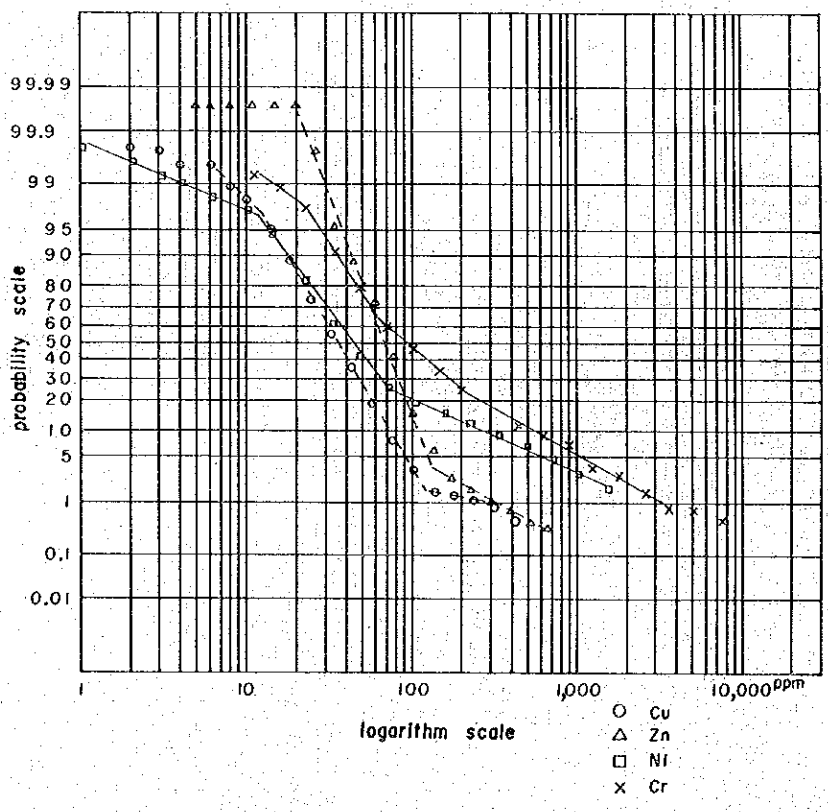

Fig. II–7 Cumulative Frequency Distribution of Each Element

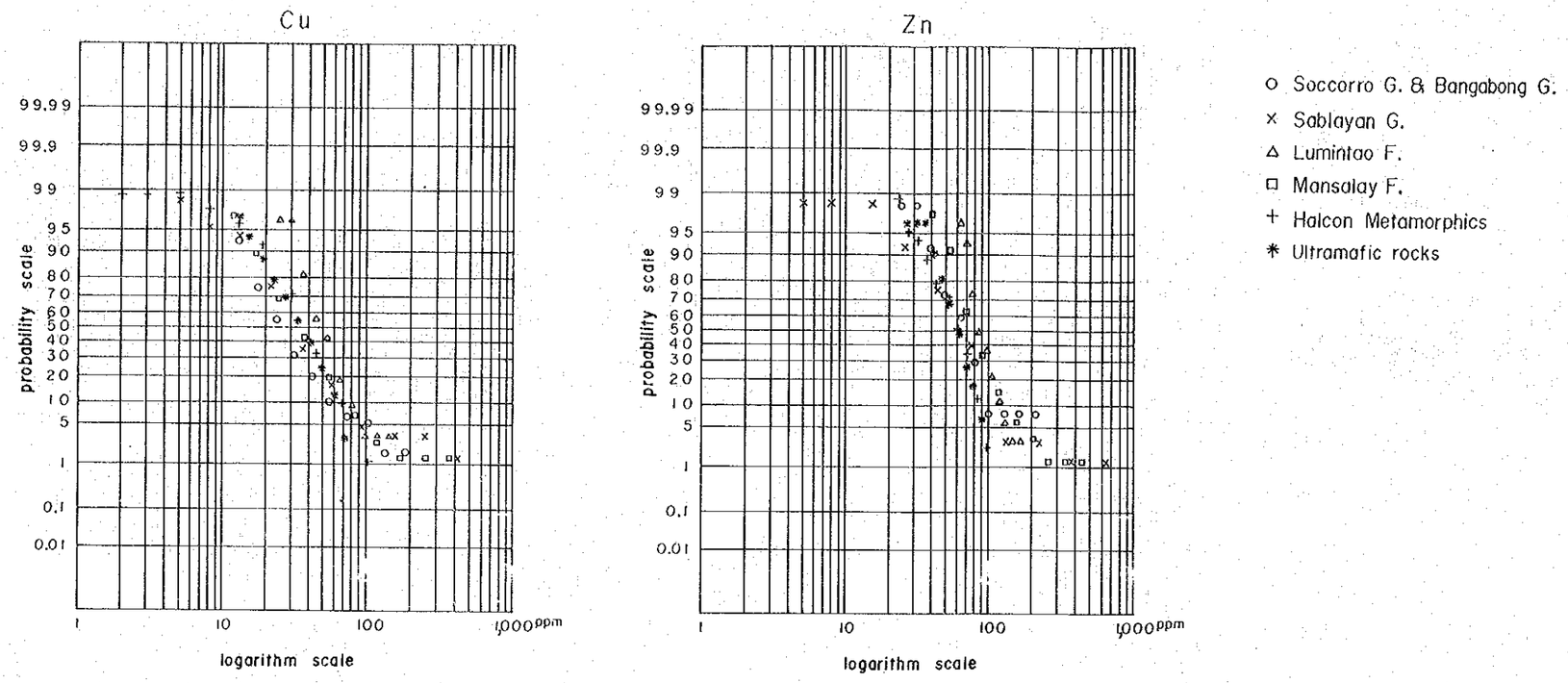

Fig. Ⅱ-6 Cumulative Frequency Distribution of Cu, Zn Ni and Cr of Each Geological Unit

and Cr have some differences by geological unit, showing high values in Ultramafic rocks and Socorro – Bongabong group, the latter of which seems to be affected by ultramafic rocks, because in most cases ultramafic rocks can be expected in the upper stream of the river where Socorro – Bongabong group is distributed.

As stated above, it becomes clear that Ni and Cr differ in their contents by geological unit. But this time the numbers of samples by the unit are not enough to treat, therefore all samples were processed collectively.

Fig. II–7 shows the cumulative frequency distribution curves by element.

Although Cu and Ni curves have break at the abscissa of around 20%, t=M+2SD was taken as the threshold value by the same consideration as the t of Cr-factor score. On the other hand, the break of Cu is below 2.5% level, so t=M+2SD was taken. As the break of Zn Curve is near 3.5% level, t=145 ppm was chosen from the figure (Fig. II–7). Concerning Ni and Cr with many high values, the distribution of high anomalous zones became clear by illustration with t'''=2.5SD.

As many analytical data of Ag are below the detectable limit that the statistical analysis of unitary element cannot be carried out, the value of 2.5% level was conveniently taken as the treshold value.

Table II–7 shows the treshold values of Ni, Cr, Zn and Ag thus calculated. Plate II–2–1 ~ 4 Geochemical Anomaly Maps were constructed based on these values. The illustration method of geochemical anomalies and cares to be paid on interpretation are the same as those in the factor map construction.

Table II–7 Regional Threshold Values of Elements

Element	t (ppm)	t''' (ppm)	Number of Anormalous Samples (pcs)	Number of Samples (pcs)
Ni	497	878	27	422
Cr	1092	1917	18	
Cu	120	–	12	
Zn	145	–	16	
Ag	0.9	–	11	

t : Threshold value

2–3–4 Interpretation of the Geochemical Anomalous Zones

Plate II–1–1 4 Factor Maps show that the anomalies of Factor 1 concentrate on the east side of the central mountain range, especially in almost all drainage systems from the Magasawangtubig River to Bongabong southward. But the anomalies in the west side are small in scale, scattering in the upstream of the Amnay River or in the midstream of the Pola River. The factor 2 anomalies occur in all drainage basin of the Rayusan River, sporadically in the area from the Bugsanga River to the Siange River, in the Malaylay River and the Pagbahan River and near the Abra de Ilog River. On comparing these anomalies with those of the unitary element analysis, Factor I anomalous zones agree well with those of Ni–Cr and Factor 2 anomalous zones, those of Cu–Zn.

Based on factor and unitary element analysis, 9 areas can be extracted as the anomalous zones, which details are as follows.

(1) Paragpagan Cr–Ni Anomaly (drainage area : 8km^2)

The anomaly extends from the branch of the Pola River to that of the Amnay River, existing in the ultramafic body extended in a NW–SE direction. Exploratory works were once carried out for nickeliferous laterite.

Contents of two samples are 728–1448 ppm Cr and 302–900 ppm Ni.

(2) Amnay River Cr–Ni Anomaly (drainage area : 5km^2)

The anomaly, covering two branches of upstream of the Amnay River, shows values of 1,143 – 2,086 ppm Cr and 732 – 1,920 ppm Ni. The exposed rocks in the area are serpentinized ultramafics. This anomaly has been newly detected this time. No exploration have been done in the area.

(3) Villacervesa Cr–Ni Anomaly (drainage area : 94km^2)

The anomaly on the west side of Villacervesa which is located in the midstream of the Magasawangtubig River show high values ranging from 1,962 to 6,466 ppm Cr and 763 – 1,722 ppm Ni. As stated in Chapter 2, Anglo Philippine Oil Corp. conducted auger-exploration in this area and secured 49,000,000 tons of nickeliferous laterite. Eagle Pass Prospect and Aglubang Prospect are also included in the anomaly.

(4) Pula River Cr Anomaly (drainage area : 3km^2)

The anomaly extending from the Pula River to the Balete River is in a small scale but

shows very high values ranging from 2,426 to 10,565 ppm. It is located about 2km apart from the Ultramafic rocks and occurrs in fine-grained tuff of Bongabong group. An unconfirmed ultramafic rock may be expected within the vicinity.

(5) Bunsud River Cr–Ni Anomaly (drainage area : 62km^2)

This anomaly extends 15km in a N–S direction, centering around the upstream of the Bansud River. The average contents of 6 stream sediment samples are 2,118 ppm Cr and 1,418 Ni. It is reported that Blueridge mining Corp. explored nickeliferous laterite in the Bongabong drainage system and got geochemical samples with 0.80 – 2.95% Ni. This prospect is included in Bansud anomaly.

(6) Rayusan Zn Anomaly (drainage area 76km^2)

This anomaly is obtained in the upstream of the Ibod River, showing not so high values ranging from 152 to 204 ppm Zn (with 39 – 158 ppm Cu). The area is composed of slate of the Mansalay formation and basalt lava of the Lumintao formation, in the former of which the anomalous values are detected. As the geological survey could not find out any mineralization, the anomaly may depend upon the lithology. But factor scores of samples are geneally high, so that a check survey on the surrounding area is needed.

(7) Siange River Cu–Zn Anomaly (drainage area : 52km^2)

The anomalous zone covering the upstream of the Bugsanga River and the Siange River, a branch of the Bongabong, show the values of 100 – 450 ppm Cu, 160 – 520 ppm Zn. At the bank of the Siange River some pyrite-quartz veinlets with a few centimenters in width occur in sandstone of Mansalay formation and silicification is widely observed. The operating barite mine is included in this zone.

(8) Alitaytayan Ag and Mongpong Ag Anomalies

As the Ag anomalous level is too low as 0.9 ppm, it is questionable to consider the values above the level to be anomalous. Alitaytayan and Mongpong anomalies, showing 1.2 – 3.2 ppm Ag, occur in limestone of Sablayan group.

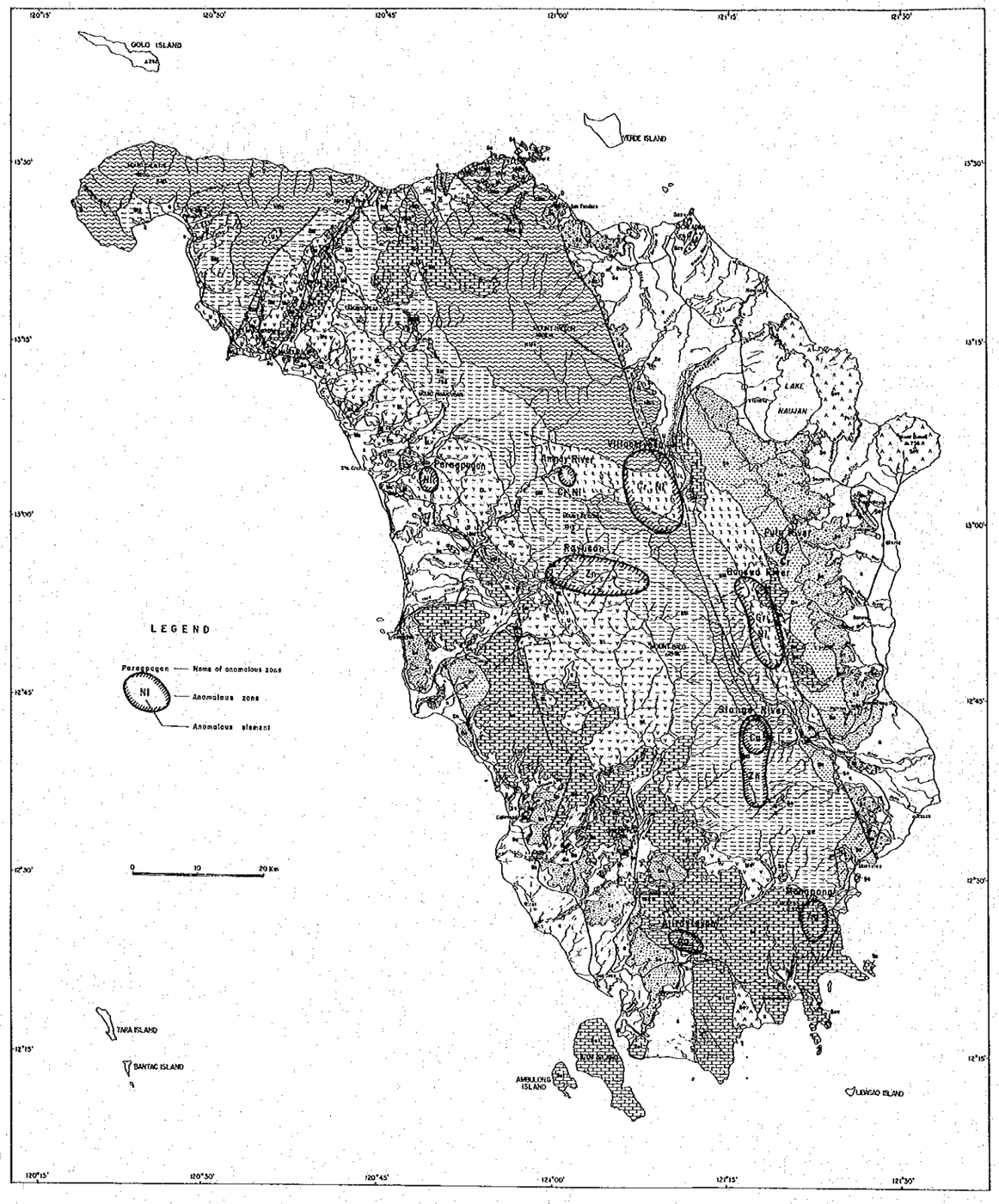

Fig. Ⅱ-8 Geochemical Anomaly Map of the Survey Area

Chapter 3 Geochemical Heavy Mineral Survey

3–1 Sampling Method

In order to determine the distribution of heavy minerals over the whole island, a program of sampling was conducted. Samples of a fixed quantity (2,000 cm^3 excluding rocks) were taken from river beds, piedmont areas, and from the larger tributaries encountered along the geological survey routes. The heavy minerals in these samples were concentrated and extracted by professional panners. A total of 105 samples were collected and treated.

3–2 Analytical Method

Several methods could have been used to separate out the heavy minerals. Two of these were considered, they are the iso-dynamic separator method, which uses the difference in magnetic characteristics of the materials to be separated, or the heavy liquid method, which uses differences in density. However, neither of these methods was used as the samples were already concentrated to a few grams by panning and the mineral identification and number of composition were directly determined by microscopic examination.

Initially the ore minerals were split into 13 types from analysis of such things as: crystal form, transparency, color and luster. Later, by the use of X-ray diffraction, and from the study of thin sections of the transparent minerals, and polished sections of the opaque minerals, the five major components, and some minor components, were determined.

The major components are as follows: magnetite, chromite, pyrite, garnet and pyroxene. The minor components are quartz plagioclase and sericite.

The weights by mineral of each sample are shown in Table A–8.

3–3 Compilation and Interpretation of the Results

Among the splitted 8 components, useful heavy minerals are magnetite, chromite and pyrite, in which interpretation was conducted.

Generally, the distributions of heavy minerals in the river bed are not uniform and are much affected by the topography of the sampling site. Besides, the weights of heavy minerals tend to be influenced by panners, because the ending time of panning is left to their judgement, therefore, instead of comparison of 3 minerals' weights, the ratio of each mineral weight to total weight of 3 minerals is calculated and showed in Plate II–3 by fan-shaped graph.

The features of distribution by mineral are as follows.

a) Chromite

There are more drainages with high percent of chromite on the east side than those on the west. On comparing two plates, Plate II–3 and Plate I–4, chromite is concentrated in the ultramafic zone, that is, high chromite concentration on the east side extending from the Bukayao River (W–149H) to the Bongabong River via the Magasawangtubig River is considered to be related with the ultramafic rocks.

On the west side, chromite distribution agrees well with the ultramafic zone in the Ibod River which is flowing to Sablayan. Anomalies, occurred in the upstream of the Malaylay River and in the area of Basement rocks between Mamburao and Paluan, suggest the existence of uncertain ultramafics.

The anomalies in Sablayan, Bongabong and Socarro groups distributed from Sablayan to Roxas via San Jose are supposed to be caused by ultramafic particles in the groups' sandstone.

(b) Magnetite

As stated before, factor analysis has disclosed the close relation between Fe and Cr in the stream sediment samples. Magnetite distribution also shows a similar tendency as chromite, with a high concentration in the ultramafic zone.

But, like in stream sediment survey any anomalies could not be obtained in the upstreams of the Mamburao and Pagbahan Rivers where some iron deposits are known and many ore floats with a size of human head are scattered.

(c) Pyrite

The percentages of pyrite are inclined to be rather high in Basement rocks. As no factor anomalies occur in the northern part of Mt. Halcon and in Paluan, pyrite concentration seems to be due to the lithology. But Rayusan Zn anomalous zone in the upstream of the Ibod River near Sablayan and Siange Cu–Zn anomalous zone extending from the upstream of the Bugsanga River to the Siange River suggest that pyrite concentration in these areas is likely related with not only lithology but also mineralization.

PART Ⅲ AIRBORNE MAGNETIC SURVEY

1 General Remarks

The airborne magnetic survey conducted over Mindoro Island, Philippines, which covers an area of 10,000 sq km, forms a part of Phase I Mineral Resources Survey of Mindoro Island, Philippines.

This report describes the procedure used for data acquisition and the results of the interpretation of the data obtained.

The data aquisition work at the field was carried out by the Bureau of Mines and Geo-Sciences (BMG), Ministry of Natural Resources, Philippines. Before the commencement of the survey, two Japanese electronic engineers were dispatched to the Philippines to check the data aquisition system of BMG, and one Japanese geophysicist stayed in the Philippines during the survey to examine the quality of the measured data and to store the read-out of analog record in magnetic tapes.

Initially, it is planned to use digital tape records to draw out the total magnetic intensity (TMI) map, but because magnetic values were not systematically or randomly stored in digital tapes, it was later decided to use the flight path maps provided by BMG and the read-out data of analog records in contouring the TMI map. Since the original analog records are not available in Japan, and therefore no re-examination of the raw data was possible.

The outline of the major structures and lineament trends were determined by the qualitative analysis with the aid of the geological information available. In central Mindoro, lineaments trending NW–NNW correspond to the major structures (faults) and the highly magnetized bodies (low anomalies) which are dominantly distributed in the NW direction coincide with the ultramafic rocks. On the other hand, lineaments trending NE–ENE characterize the northwestern part.

2 Outline of Airborne Magnetic Survey

2–1 Survey Area

The airborne magnetic survey described in this report was carried out in the area as shown in Fig. III–1.

The area analyzed forms a polygon whose apexes are listed below;

A :	13°35'N, 120°15'E	B :	13°35'N, 120°47'E
C :	13°35'N, 120°50'E	D :	13°35'N, 121°05'E
E :	13°23'N, 121°20'E	F :	13°19'N, 121°24'E
G :	13°10'N, 121°35'E	H :	12°30'N, 121°35'E
I :	12°19'N, 121°35'E	J :	12°16'N, 121°20'E
K :	12°10'N, 121°15'E	L :	12°10'N, 121°00'E
M :	12°34'N, 120°50'E	N :	12°41'N, 120°45'E
O :	12°45'N, 120°45'E	P :	12°55'N, 120°45'E
Q :	13°20'N, 120°25'E	R :	13°20'N, 120°15'E

Mountains of higher than 1,800m above sea level (A.S.L.), specifically Mt. Halcon (2,582m) and Mt. Baco (2,488m), are prominent in the central part of Mindoro Island, so two flight altitudes, i.e., 1,800m (6,000 ft) A.S.L. and 2,700m (9,000 ft) A.S.L., were adapted. The area flown at 1,800m A.S.L. are the western side (A–B–C–M–N–O–P–Q–A) and the eastern side (E–F–G–H–I–J–E) of Mindoro Island. The central portion (B–C–D–E–F–I–J–K–L–M–N–B) was flown at 2,700m A.S.L.

2–2 Survey Period

Checking of the data aquisition equipments of the airborne magnetic survey was done from February 8 to February 15, 1982.

Data acquisition work was carried out by the Bureau of Mines and Geo-Sciences, from February 20 to April 17, 1982.

One Japanese geophysicist was dispatched to the Philippines during the period March 8 through April 23, 1982 to check the quality of the measured data and to do preliminary data processing.

Data processing and analyses were conducted during the period April 26 through August 31, 1982.

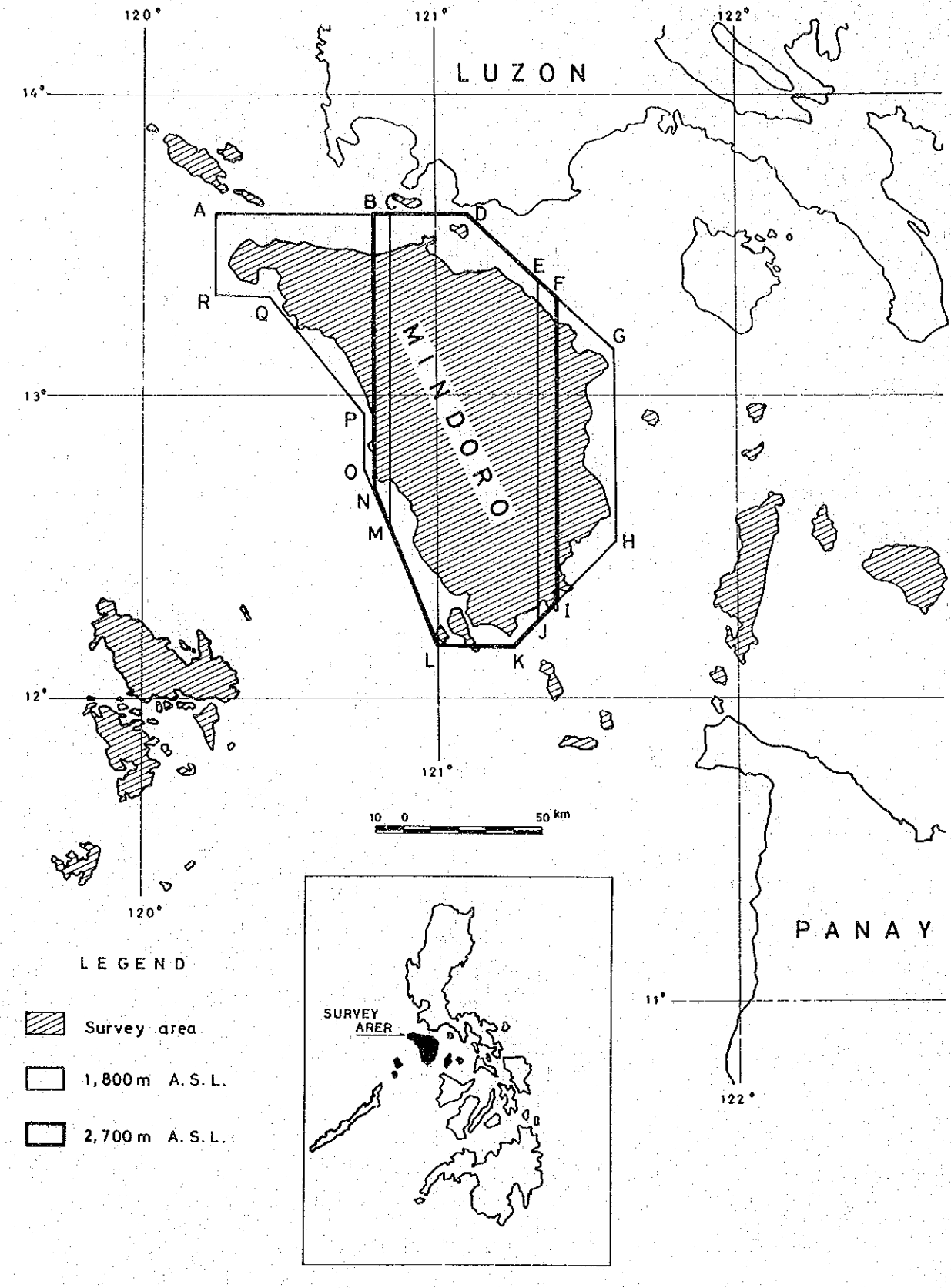

Fig. Ⅲ-1 Location Map of the Survey Area

2–3 Member of the Survey

Checking of the instruments :

Asahi Hattori	Carlos F. Teodoro
Yoshinori Azuma	Romeo B. ZAzambarrano
Yaichi Tanaka	Enrico B. Zuno

Field survey :

Manabu Kaku	Octavio C. Daclison
	Alexander M. Lacanilao
	Reynaldo L. Villela
	Romeo B. Zambarrano
	Enrico B. Zuno
	Honorio B. Cabanban
	Elmer C. Amo

Data processing and analyses :

Asahi Hattori	Octavio C. Daclison
Susumu Sasaki	Macario A. Del Rosario
Manabu Kaku	Alexander M. Lacanilao

2–4 Summary of Field Operations

The present field work was dealt with as follows;

(1) Airbase : San Jose Airport, Mindoro Island

(2) Ground Station : San Jose, Mindoro Island

(3) Total Survey Area : 10,000 sq km

(4) Flight Altitude : 1,800m (6,000 ft) A.S.L. and 2,700m (9,000 ft) A.S.L.

(5) Flight Line Spacing : 2.5km for the traverse lines and 10 km for the tie lines

(6) Flight Direction : NS and EW

(7) Number of Flight Lines

	1,800 mA.S.L.	2,700 mA.S.L.	Total
Traverse line	31	29	60
Tie line	18	14	32

(8) Lengths of Lines

	1,800 mA.S.L.	2,700 mA.S.L.	Total
Traverse line	1,590 km	3,601 km	5,191 km
Tie line	379 km	800 km	1,179 km
Total	1,969 km	4,401 km	6,370 km

(9) Geomagnetic Dip : 14°N

(10) Geomagnetic Declination : 0°

(11) Total Geomagnetic Intensity : 40,000 gammas

2–5 Survey Instrumentation and Method of Survey

The instrumentation system used in the survey which belongs to the Bureau of Mines and Geo-Sciences are as follows:

(a) Aircraft : Cessna 402, twin-engine

(b) High Sensitivity Airborne Proton Magnetometer : V–4914 made by Varian (USA)

(c) High Sensitivity Station Proton Magnetometer : G–826A made by Geometrics (USA)

(d) Crystal Clock : GP–109 made by Varian (USA)

(e) Barometric Altimeter : 5934A–A69 made by United Instrument (USA)

(f) 35mm Tracking Camera : G–2 made by AUTOMAX (USA)

(g) Analog Recorder : 680 made by Hewlett-Packard (USA)

(h) Digital Data Acquisition System : V–4991 made by Varian (USA)

Navigation of this survey was done visually, comparing prominent land marks with 1:50,000 scale topographic maps (also called pilotage maps). It is difficult to fly exactly over the planned survey lines. If the spacing between neighboring flight paths is greater than twice of the planned line spacing, then re-flights are made.

If there is a large accumulation of clouds in the survey area, no flights are made since it would be very difficult to navigate visually and the tracking camera would only photograph clouds.

The average speed of the aircraft is 130 mph (about 240 km/h) and the sampling interval of the airborne magnetometer is four (4) seconds.

2–6 Data Processing

2–6–1 Flight Path Map

The determination of flight path was made by using tracking films, at the field. Since the time to project the tracking film was limited due to the electric power condition at San Jose (the electricity was supplied only at night time), the completion of the flight path map was considerably delayed.)

The procedure of mapping the flight path maps are as follows;

(1) Tracking films are developed and dried on the same day after survey flight.

(2) Fiducial points are marked on the 35mm tracking film and are magnified by means of the magnifier/viewer and the plotted points on the film are transcribed on the maps of scale 1:50,000.

(3) Using these flight path maps, flight plan of next day, additional flight lines and re-flight are decided.

(4) When the survey is completed and all fiducial points have been drawn in the topographic map, the outline of the survey area and the flight paths are traced and white printed.

2–6–2 Diurnal Correction for Geomagnetic Field

Ground station geomagnetic measurements were continuously carried out at San Jose, Mindoro Island, to monitor the diurnal magnetic variations to be applied to the airborne magnetic data and for the observation of magnetic storms.

Magnetic storm and/or sudden geomagnetic change were observed twice during the survey period, and the data measured on the same days were discarded and the lines were re-flown.

The mean total intensity of the geomagnetic field amounted to 39,600 gammas at the ground magnetometer station. The correction table of diurnal variation was made on the basis of the analog records of time variations from the mean total intensity. The aeromagnetic data were corrected in reference to the correction table, and then final data without any time effect were obtained.

2–6–3 Total-Intensity Map

After the daily-variation corrections, the airborne magnetic data were transcribed on the 10-second interval reference marks plotted on the flight path map. It is sometimes seen that some differences between magnetic values occur at intersection points of traverse lines and tie lines. Possible causes of errors may be due to positioning, flight altitude and heading of air-

craft (heading error is a magnetic change induced by change in flight direction). In case there is any magnetic closing-error at the intersection point of traverse and tie lines, the positioning and the horizontality of the aircraft are re-examined. The closing errors were minimized in a least-squares sence. Finally, the total intensity map was drawn on the basis of the data given at the grid points.

As mentioned in 2–1, in this survey, two flight altitudes, i.e., 1,800 mA.S.L. and 2,700m A.S.L., were adapted so that total intensity data for former's level were obtained at 0.5km grid and for latter's level at 1km grid spacing. Then two separate intensity maps were drawn at the contour interval of five gammas.

2–6–4 Residual Map

The residual map was drawn at the contour interval of five gammas on the basis of the geomagnetic regional field, which was calculated by subtracting the standard total intensity of the International Geomagnetic Reference Field (IGRF) from the interpolated intensity values at grid points.

2–7 Method of Analysis

Aeromagnetic data in the form of a residual map can be analyzed by two methods, qualitative analysis and quantitative analysis.

The first is a qualitative speculation of geological features selectively extracted from geomagnetic residual anomalies by means of some filtering procedures. The filters generally used are given as follows:

(1) Band-pass filter: which selectively extracts the magnetic anomalies with the optional region of wave length.

(2) Second vertical derivative filter: which emphasizes the short-wavelength magnetic anomaly, and is used to delineate the magnetized bodies.

(3) Upward or downward continuation filter: which attennuates or emphasizes the short wavelength magnetic anomalies by calculating the magnetic values on the upper or lower level mathematicaly.

(4) Auto-correlation analysis: which delineates the geomagnetic characteristics by detecting similar magnetic anomalies.

(5) Spectral analysis: which is to understand the wavelength characteristics of the geomagnetic anomalies in the survey area.

(6) Reduction-to-pole filter: which is used to infer the shape of the magnetized body by calculating the magnetic anomaly at the magnetic pole mathematically.

The second analysis aims to estimate the depths, shapes and magnetic properties of magnetized bodies. The corresponding methods are as follows:

(1) Specific Point Method: Method for estimating the depth or width of a magnetized body from the location of specific points of magnetic anomaly curves.

(2) Curve Matching Method: Method for calculating the susceptibility, depth, width, length and geometrical dip of magnetized body by comparing the observed anomaly with theoretical anomaly generated by simple models (sphere, cylinder, dike and prism) and their combinations.

(3) Specific Curve Method: Method for estimating the depth or width of a magnetized body from the location of the curvature of observed anomaly curves.

(4) Analytical Method: Method for the determination of depth, geometrical dip and magnetic properties of magnetic structures (like dike and/or step) by comparing the theoretical spectral characteristics with the spectral characteristics of the observed magnetic profiles calculated by Fourier (or Fourier-Hilbert) transform.

In this survey, residual map of the whole survey area was not obtained because aeromagnetic survey was conducted at two different altitudes, i.e. 1,800 mA.S.L. and 2,700 mA.S.L. as mentioned in 2–1.

Residual map covering the whole area will be made by compiling the residual map of 2,700 mA.S.L. with the upward-continuated residual map (from 1,800 mA.S.L. to 2,700 mA.S.L.) of western and eastern Mindoro.

The coefficient tables of upward-continuation filter used are shown in Table III–1.

For actual computations, discrete data for 1,800 mA.S.L. residual map are taken at 0.5km grid points. Upward-continuated values to 2,700 mA.S.L. are obtained by means of the convolution between these discrete data and filter coefficients as given in Table III–1. Since many points will be discarded at the marginal zone of the residual map after computation, the small operators as shown in the lower portion of Table III–1 will be employed.

The energy spectrum analysis by two-dimensional Fourier transform will be applied to the magnetic data of over 64km x64km of the survey area flown at 2,700 mA.S.L. in the vicinity of Mt. BAco. From the wavelength characteristics, band-pass filtered map will be obtained from the residual map. Finally, these maps including the residual map should be considered as the basis for